Journal of Mathematical Chemistry (2022) 60:1930–1982
https://doi.org/10.1007/s10910-022-01397-w

ORIGINAL PAPER

Solution of the modified Yukawa–Kratzer potential under influence of the external fields and its thermodynamic properties

Kaushal R. Purohit[1] · **Rajendrasinh H. Parmar**[2] · **Ajay Kumar Rai**[1]

Received: 27 February 2022 / Accepted: 11 August 2022 / Published online: 6 September 2022

Abstract

The Schrödinger equation has been solved in two dimensions for the modified Yukawa–Kratzer potential (MYKP) under the influence of the magnetic field and the Aharanov–Bohm flux field (external fields). The energy eigenvalues and wave function were calculated using the parametric Nikiforov–Uvarov approach. From the resulting energy eigensolution of MYKP, we calculated energy eigenvalues for generalised Kratzer potential (GKP), modified Kratzer potential (MKP), Kratzer potential (KP), and Hellmann potential (HP). The energy values for MYKP, KP, MKP, and GKP are tabulated numerically. Under the impact of external fields, we explore different thermodynamic parameters such as partition function, mean energy, mean free (internal) energy, entropy, specific heat capacity, magnetization at finite temperature, and magnetic susceptibility at finite temperature. Plots of the effective potential, energy eigenvalues, and thermodynamic properties for various parameters were provided. The calculated numerical results for KP and HP under the effect of the magnetic field and the Aharanov–Bohm flux field are quite close to those obtained by others. In addition, MYKP also solves the Schrödinger equation using the series expansion method. It is possible to get confined state energy spectra. For distinct n,m quantum numbers for $q = 1$, numerical values of energy spectra of special cases Kratzer potential for N_2 and CH molecules are computed, and the findings are consistent with NU method.

Keywords Modified Kratzer potential · Modified Yukawa potential · Magnetic field · Aharanov–Bohm flux field · Parametric Nikiforov–Uvarov method · Series expansion method

✉ Kaushal R. Purohit
kaushalsep1996@gmail.com

[1] Department of Physics, Sardar Vallabhbhai National Institute of Technology, Surat, Gujarat 395 007, India

[2] Sir P T Science College, Modasa, Gujarat 383 315, India

1 Introduction

The schrödinger equation or schrödinger type equation can be solved analytically or numerically to offer us a lot of information about a physical system. Because of their importance in statistical physics, solid-state physics, quantum field theory, and molecular physics, researchers are interested in solving these types of equations in the relativistic and non-relativistic regimes. Since the last decade, many researchers have been working to solve the diverse physical potentials in two dimensions under the influence of the magnetic field and the Aharanov–Bohm flux field for both relativistic and non-relativistic realms [1–4].

Different methods are available in the literature to solve second order differential equations, including: Nikiforov–Uvarov (NU) method [5–7], exact quantization rule [8–11], Qiang-Dong proper quantization rule [12, 13], the path integral method [14], asymptotic iteration method (AIM) [15], factorization method [16], Laplace transform approach [17], supersymmetric quantum mechanics (SUSYQM) [18, 19], ansatz method [20] and series expansion method [21]

Spectral features of an electron in a two-dimensional (2D) Gaussian quantum dot (GQD) investigated by Aalu [22] through the Nikiforov–Uvarov method under the combined action of magnetic field, electric field, and AB flux field. Many researchers have investigated quantum rings in the presence of an external magnetic field, observing new phenomena such as spin orbit [23], quantum hall [24], Berry's phase [25], persistent currents [26], and the Aharonov–Bohm [27]. Ikot et al. [28] examined different thermodynamic features in the framework of superstatistics, employing the pseudoharmonic potential under the influence of external magnetic and AB fields. Ikot et al. [29] solved the screened Kratzer potential in two dimensions under the influence of the magnetic field and the Aharanov–Bohm flux field and examined various thermodynamical features. Ikhdair et al. [30, 31] investigated 2D harmonic and pseudo-harmonic oscillators in the presence of external fields and got the energy spectrum and wave function of an electron. Hamzavi et al. [32] explored the spin and pseudospin symmetry for the Killingbeck potential using a quasi-exact solution. The quark-antiquark interaction Killingbeck potential was solved using the power series technique under the effect of external fields [33, 34]. Ikhdair et al. [35] investigated non-relativistic molecular models in the presence of external magnetic fields.

Ibekwe et al. [36] analytically solved the radial Schrodinger equation with an exponential, generalised, anharmonic Cornell and created the mass spectra of the heavy quarkonium system. Theoritically Quarkonia physics now a days very important due to many available experimental states [37–40]. Using the WKB approach, Omugbe et al. [41] calculated the mass spectrum of mesons. In nuclei, atoms, molecules, and spectroscopy, as well as many other fields of physics, the accurate solution of the Schrodinger equation with some solvable potential plays an important role [42]. Obtaining analytical solutions to the radial schrödinger equation with the provided interaction potential without the use of approximation approaches is a difficult task. Ibekwe et al. [43] obtained mass spectra of heavy quarkonium for screened Kartzer potential using series expantion method. The nature of the potential model influences the applications of Schrödinger equation solutions in various circumstances [44]. AbuShady and Ezz-Alarab [45] employed an exact-analytical iteration method

to study the N-radial Schrödinger equation analytically and used the results to compute the thermodynamic properties and mass of mesons. The energy eigenvalues and normalised eigen-functions of the radial SE in N-dimensional space for the quark–antiquark interaction potential were calculated analytically by Kumar and Fakir [46].

Purohit et al. [47] investigated the thermodynamic parameters of the filtered cosine Kratzar potential in the presence of a magnetic field and an Aharanov–Bohm flux field.

The modified Yukawa–Kratzer potential (MYKP) [48] solved in this study under the effect of the magnetic field and the Aharanov–Bohm flux field written as,

$$V(r) = \frac{a_1 e^{-2\alpha r}}{r^2} - \frac{a_2 e^{-\alpha r}}{r} + a + D_e - \left(\frac{A_1}{r} - \frac{A_2}{r^2}\right) \tag{1}$$

where $A_1 \equiv 2D_e r_e$, $A_2 \equiv D_e r_e^2$. r_e is the equilibrium bond length the interatomic distance r, α are the screening parameters, and D_e is the dissociation energy.

In the non relativistic framework, Parmar et al. [48] achieved the solution to MYKP using the Nikiforov–Uvarov (NU) method and the SUSYQM method. They look into several thermodynamical parameters, expectation values utilising the Hellmann–Feynman theorem, and the eigensolution of the chosen dimer inferred from MYKP eigensolutions.

In this paper, we used the parametric Nikiforov–Uvarov (pNU) approach to determine the eigenspectrum of the MYKP Eq. (1) under the effect of the magnetic field $\vec{B}$ along the z direction and the Aharanov–Bohm flux field Φ_{AB} formed by a solenoid. The energy eigenvalues spectrum of the MYKP is computed numerically for various values of the magnetic field $\vec{B}$ and Aharanov–Bohm flux field Φ_{AB}. By setting potential parameters, we deduced generalized Kratzer potential, modified Kratzer potential, Kratzer potential, and Hellmann potential and its energy spectrum using energy spectrum of MYKP. Different thermodynamic properties such as partition function $Z(\vec{B}, \Phi_{AB}, \beta)$ mean energy $U(\vec{B}, \Phi_{AB}, \beta)$, mean free energy $F(\vec{B}, \Phi_{AB}, \beta)$, entropy $S(\vec{B}, \Phi_{AB}, \beta)$, specific heat capacity $C_s(\vec{B}, \Phi_{AB}, \beta)$, magnetization $M(\vec{B}, \Phi_{AB}, \beta)$ at finite temperature and magnetic susceptibility $\chi_m(\vec{B}, \Phi_{AB}, \beta)$ at finite temperature for MYKP is presented. Plots of the effective potential and energy eigenvalues are also addressed with respect to α, magnetic field $\vec{B}$, and Aharanov–Bohm flux field Φ_{AB}. We also looked at graphs of thermodynamic properties vs various parameters. We used $m \to (D-2)/2 + \ell$ to extend our work to D dimensions, where m and ℓ are magnetic and angular quantum numbers, respectively. We also used the series expansion method to solve MYKP and obtain energy spectra, which we compared to the NU method for a few dimers.

This is how the article is structured: The pNU technique is explained in Sect. 2. In Sect. 3, we presented the MYKP solution obtained under the effect of the magnetic field and the Aharanov–Bohm flux field. Section 4 presents solution of the MYKP using series expansion method and obtained thermodynamic properties. Section 5 presents the results and discussions. A brief conclusion is presented in Sect. 6.

2 Review of the parametric Nikiforov–Uvarov (pNU) method

The generalized form of the Schrödinger like second order differential equation for any potential written as [28, 49],

$$\frac{d\Psi(u)}{du^2}+\frac{g_1-g_2u}{u(1-g_3u)}\frac{d\Psi}{du}+\frac{-B_1u^2+B_2u-B_3}{u^2(1-g_3u)^2}\Psi(u) \tag{2}$$

From the parametric Nikiforov–Uvarov (pNU) method, the energy eigenvalues and eigen functions respectively become [28, 49]

$$\begin{aligned}&(g_2-g_3)n+g_3n^2-(2n+1)g_5+(2n+1)\left(\sqrt{g_9}+g_3\sqrt{g_8}\right)\\&+g_7+2g_3g_8+2\sqrt{g_8g_9}=0\end{aligned} \tag{3}$$

$$\Psi(u)=u^{g_{12}}(1-g_3u)^{-g_{12}-\frac{g_{13}}{g_3}}P_n^{(g_{10}-1,(g_{11}/g_3)-g_{10}-1)}(1-2g_3u) \tag{4}$$

where

$$g_4=(1-g_1)/2,\quad g_5=(g_2-2g_3)/2,\quad g_6=g_5^2+B_1,\quad g_7=2g_4g_5-B_2,\quad g_8=g_4^2+B_3$$
$$g_9=g_3g_7+g_3^2g_8+g_6,\quad g_{10}=g_1+2g_4+2\sqrt{g_8},\quad g_{11}=g_2-2g_5+2(\sqrt{g_9}+g_3\sqrt{g_8})$$

$$g_{12}=g_4+\sqrt{g_8},\quad g_{13}=g_5-(\sqrt{g_9}+g_3\sqrt{g_8}) \tag{5}$$

for $g_3=0$,

$$\lim_{g_3\to 0}P_n^{(g_{10}-1,(g_{11}/g_3)-g_{10}-1)}(1-2g_3u)=L_n^{g_{10}-1}(g_{11}u) \tag{6}$$

and

$$\lim_{g_3\to 0}(1-g_3u)^{-g_{12}-\frac{g_{13}}{g_3}}=e^{g_{13}u} \tag{7}$$

Equation (4) becomes

$$\Psi(u)=u^{g_{12}}e^{g_{13}u}L_n^{g_{10}-1}(g_{11}u) \tag{8}$$

where $L_n^{g_{10}-1}(g_{11}u)$ is Laguerre polynomials.

3 Eigensolution of the MYKP with an external fields

A general formalism of the Schrödinger equation for a charged particle moving under the influence of the vector potential $\vec{A}$ written as

$$\left[\frac{1}{2\mu}\left(\vec{p}+\frac{q}{c}\vec{A}\right)^2+V(r)-E_{nm}\right]\psi(r,\phi)=0 \tag{9}$$

where μ-reduced mass of the system and q is the charge of the particle, E_{nm} energy eigenvalues, vector momentum $\vec{p} = -i\hbar\vec{\nabla}$, c velocity of light, vector potential $\vec{A} = (A_r, A_\phi, A_z)$, and $V(r)$ scalar potential and wave function $\psi(r,\phi) = (2\pi r)^{-1/2} e^{im\phi} G_{nm}(r)$. For $\vec{A}_r = \vec{A}_z = 0$, $\vec{A} = (0, A_1 + A_2, 0)$. A vector potential $\vec{A}$ can be expressed as $\vec{A} = \vec{A}_1 + \vec{A}_2$ with $\vec{\nabla} \times \vec{A}_1 = \vec{B}$ and $\vec{\nabla} \times \vec{A}_2 = 0$
where $\vec{B}$ is applied magnetic field and $\vec{A}_2$ presenting AB flux field Φ_{AB} arise due to the uniform magnetic field. Where $\vec{A}_1$ and $\vec{A}_2$ written as [50, 51]

$$\vec{A}_1 = \frac{\vec{B}e^{-\alpha r}}{1-e^{-\alpha r}}\hat{\phi} \text{ and } \vec{A}_2 = \frac{\Phi_{AB}}{2\pi r}\hat{\phi} \text{ therefore}$$
$$\vec{A} = A_1 + A_2 = \left(\frac{\vec{B}e^{-\alpha r}}{1-e^{-\alpha r}} + \frac{\Phi_{AB}}{2\pi r}\right)\hat{\phi} \tag{10}$$

where $\Phi_{AB} = 2\pi q^{-1}$. Inserting Eqs. (1) and (10) into Eq. (9), we obtain

$$\left[\nabla^2 - \frac{q^2}{\hbar^2 c^2}\left(\frac{\vec{B}e^{-\alpha r}}{1-e^{-\alpha r}} + \frac{\Phi_{AB}}{2\pi r}\right)^2 - \frac{1}{\hbar^2}\left(\frac{q}{c}\vec{p}.\vec{A} + \frac{q}{c}\vec{A}.\vec{p}\right)\right]\psi(r,\phi) -$$

$$\frac{2\mu}{\hbar^2}\left(a + D_e + \frac{a_1 e^{-2\alpha r}}{r^2} - \frac{a_2 e^{-\alpha r}}{r} - \frac{A_1}{r} + \frac{A_2}{r^2} - E_{nm}\right)\psi(r,\phi) = 0 \tag{11}$$

Using Greene–Aldrich approximation [52]

$$\frac{1}{r^2} \approx \frac{\alpha^2}{(1-e^{-\alpha r})^2}, \Rightarrow \frac{1}{r} \approx \frac{\alpha}{(1-e^{-\alpha r})}$$
$$\times \frac{d^2 F_{nm}(r)}{dr^2} + \left[\left(\mu_1(E_{nm} - a - D_e) - \frac{\mu_1 \alpha^2 a_1 e^{-2\alpha r}}{(1-e^{-\alpha r})^2}\right.\right.$$
$$\left.\left. + \frac{\mu^{'}\alpha\left(a_2 e^{-\alpha r} + A_1\right)}{(1-e^{-\alpha r})} - \frac{\mu^{'}\alpha^2 A_2}{(1-e^{-\alpha r})^2}\right)\right] F_{nm}(r) - q_1\left(\frac{2m\alpha\vec{B}e^{-\alpha r} + q_1\vec{B}^2 e^{-2\alpha r}}{(1-e^{-\alpha r})^2}\right)$$
$$F_{nm}(r) - \left[\frac{\alpha^2\left(m^{'2} - \frac{1}{4}\right) + 2q_1\alpha\vec{B}\eta e^{-\alpha r}}{(1-e^{-\alpha r})^2}\right] F_{nm}(r) = 0 \tag{12}$$
$$-\frac{d^2 F_{nm}(r)}{dr^2} + V_{eff}(r) F_{nm}(r) = \mu_1(E_{nm} - a - D_e) F_{nm}(r) \tag{13}$$

where

$$V_{eff} = \frac{\beta_1 e^{-2\alpha r} + \beta_2 e^{-\alpha r} + \beta_3}{(1-e^{-\alpha r})^2} \tag{14}$$

and $q_1 = \frac{q}{\hbar c}$, $\mu_1 = \frac{2\mu}{\hbar^2}$, $m' = m + \eta$, $\eta = \frac{\Phi_{AB} q}{2\pi\hbar c} = \frac{\Phi_{AB}}{\Phi_o}$, flux quanta $\Phi_o = \frac{hc}{q}$

$$\beta_1 = \mu_1(\alpha^2 a_1 + \alpha a_2) + \vec{B}^2 q'^2;\ \beta_2 = \mu_1\alpha(A_1 - a_2) + 2\alpha q_1(m+\eta);$$
$$\beta_3 = \alpha^2\left(m'^2 - \frac{1}{4}\right) + \mu_1\alpha(\alpha A_2 - A_1) \tag{15}$$

Equation (12) can be written as

$$\frac{d^2F_{nm}(r)}{dr^2} + \left[-\left(E'_{nm} + \beta_1\right)e^{-2\alpha r} + \left(2E'_{nm} - \beta_2\right)e^{-\alpha r} - \left(E'_{nm} + \beta_3\right)\right]F_{nm}(r) = 0 \tag{16}$$

where $E'_{nm} = -\mu_1(E_{nm} - a - D_e)$. Now using transformation $u = e^{-\alpha r}$, we get

$$\frac{d^2F_{nm}(u)}{du^2} + \frac{(1-u)}{u(1-u)}\frac{dF_{nm}(u)}{du} + \frac{1}{u^2(1-u)^2} \times \left[-(\varepsilon^2_{nm} + \xi_1)u^2 + (2\varepsilon^2_{nm} - \xi_2)u - (\varepsilon^2_{nm} + \xi_3)\right]F_{nm}(u) = 0 \tag{17}$$

$$\varepsilon^2_{nm} = \frac{E'_{nm}}{\alpha^2} = -\frac{2\mu(E_{nm} - a - D_e)}{\hbar^2\alpha^2};$$

$$\xi_1 = \frac{\beta_1}{\alpha^2} = \frac{2\mu}{\hbar^2\alpha^2}(\alpha^2 a_1 + \alpha a_2) + \frac{q^2}{\hbar^2 c^2\alpha^2}\vec{B}^2 \tag{18}$$

$$\xi_2 = \frac{\beta_2}{\alpha^2} = \frac{2\mu}{\hbar^2\alpha^2}(\alpha\,(A_1 - a_2) + \frac{2\mu}{\hbar^2\alpha^2}\left(2\alpha\vec{B}\right)(m+\eta)\,,$$

$$\xi_3 = \frac{\beta_3}{\alpha^2} = m'^2 - \frac{1}{4} + \frac{2\mu}{\hbar^2\alpha^2}(\alpha^2 A_2 - \alpha A_1) \tag{19}$$

Using Eqs. (3) and (5), we obtain

$$\sqrt{\varepsilon^2_{nm} + \xi_3} = -\frac{\left(n^2 + n + \frac{1}{2} + (2n+1)\sqrt{\xi_1 + \xi_2 + \xi_3 + \frac{1}{4}} + \xi_2 + 2\xi_3\right)}{2\left(n + \frac{1}{2} + \sqrt{\xi_1 + \xi_2 + \xi_3 + \frac{1}{4}}\right)} \tag{20}$$

Using Eqs. (18) and (19), we obtain

$$E_{nm} = a + D_e + \frac{\hbar^2\alpha^2}{2\mu}\xi_3 - \frac{\hbar^2\alpha^2}{2\mu}\left[\frac{\xi_3 - \xi_1}{2(n+\Omega)} + \frac{(n+\Omega)}{2}\right]^2 \tag{21}$$

$$E_{nm} = a + D_e + \frac{\hbar^2\alpha^2}{2\mu}\left(m'^2 - \frac{1}{4}\right) + \alpha^2 A_2 - \alpha A_1$$

$$-\frac{\hbar^2\alpha^2}{2\mu}\left[\frac{\frac{2\mu}{\hbar^2}\left(A_2-a_1-\frac{\alpha A_1-a_2}{\alpha}\right)-\frac{q^2}{\hbar^2c^2\alpha^2}\vec{B}^2+m'^2-\frac{1}{4}}{2(n+\Omega)}+\frac{(n+\Omega)}{2}\right]^2 \tag{22}$$

where

$$\begin{aligned}\Omega &= \frac{1}{2}+\sqrt{\xi_1+\xi_2+\xi_3+\frac{1}{4}}\\ &= \frac{1}{2}+\sqrt{\frac{2\mu(a_1+A_2)}{\hbar^2}+\frac{q^2}{\hbar^2c^2\alpha^2}\vec{B}^2+\frac{q}{\hbar c\alpha}2\vec{B}m'+m'^2}\end{aligned} \tag{23}$$

setting $m = K + 1/2 = \ell + \frac{(D-2)}{2}$, Eq. (22) convert into D dimensional energy eigenvalues of MYKP without an external fields reads

$$\begin{aligned}E_{n\ell} &= a + D_e + \frac{\hbar^2\alpha^2}{2\mu}K(K+1)+\alpha^2A_2-\alpha A_1\\ &-\frac{\hbar^2\alpha^2}{2\mu}\left[\frac{\frac{2\mu}{\hbar^2\alpha^2}\left(\alpha^2A_2-\alpha A_1-\alpha a_2\right)+K(K+1)]}{2(n+\Omega_1)}+\frac{(n+\Omega_1)}{2}\right]^2\end{aligned} \tag{24}$$

where

$$K = \ell + \frac{(D-3)}{2} \text{ and } \Omega_1 = \frac{1}{2}+\sqrt{\frac{2\mu(a_1+A_2)}{\hbar^2}+\left(K+\frac{1}{2}\right)^2} \tag{25}$$

Above Eq. (24) is exactly the same energy eigenspectrum obtained by Parmar et al. [48] for MYKP. From Eq. (4), the unnormalized wave function corresponds to the energy eigenvalues Eq. (22),

$$F_{nm}(u) = u^{\sqrt{\varepsilon_{nm}^2+\gamma_3}}(1-u)^{\Omega}\,{}_2F_1(-n, n+2\sqrt{\varepsilon_{nm}^2+\gamma_3}+2\Omega, 2\Omega+1; u) \tag{26}$$

In terms of the Jacobi polynomials wave function $F_{nm}(u)$ can be expressed as

$$F_{nm}(u) = N_{n\ell}\,u^{\omega}(1-u)^{\Omega}P_n^{2\omega,2\Omega-1}((1-2u);\omega=\sqrt{\varepsilon^2+\xi_3} \tag{27}$$

and $P_n^{(2\omega,2\Omega-1)}(1-2u)$ is the Jacobi polynomial which is defined as [53]

$$P_n^{(2\omega,2\Omega-1)}(1-2u) = \frac{\Gamma(n+2\omega+1)}{n!\Gamma(2\omega+1)}\,{}_2F_1(-n, n+2\omega+2\Omega, 2\omega+1; u)$$

where N_{nm} is normalization constant. Equations (24) and (27) is the energy spectrum and eigenfunction for MYKP respectively. Equation (26) can be written in terms of

hypergeometric function as

$$F_{nm}(u) = N_{n\ell}u^{\omega}(1-u)^{\Omega}\frac{\Gamma(n+2\omega+1)}{n!\Gamma(2\omega+1)}\,{}_2F_1(-n, n+2\omega+2\Omega, 2\omega+1; u) \tag{28}$$

Now, the total wave function becomes

$$\psi(r,\phi) = \frac{N_{nm}}{\sqrt{r}}e^{im\phi}e^{-\alpha\omega r}(1-e^{-\alpha r})^{\Omega} \frac{\Gamma(n+2\omega+1)}{n!\Gamma(2\omega+1)}\,{}_2F_1(-n, n+2\omega+2\Omega, 2\omega+1; e^{-\alpha r}) \tag{29}$$

4 Solution of the MYKP using series expansion method (SEM)

From Equation (13), we consider the radial Schrodinger equation [36, 44]

$$\frac{d^2u_{nm}(r)}{dr^2} + \frac{2}{r}\frac{du_{nm}(r)}{dr} + \left[-E_{nl}^{'} - V_{eff}(r)\right]u_{nm}(r) = 0 \tag{30}$$

where r is internuclear separation and E denotes the energy eigenvalues of the system. We put $F_{nm}(r) = u_{nm}(r)$ and

$$V_{eff} = \frac{1}{r^2\alpha^2}\left[\beta_1 e^{-2\alpha r} + \beta_2 e^{\alpha r} + \beta_3\right] \tag{31}$$

$$V_{eff} = \frac{\beta_1}{r^2\alpha^2} - \frac{2\beta_1}{r\alpha} + 2\beta_1 - \frac{4}{3}\beta_1\alpha r + \frac{\beta_2}{r^2\alpha^2} - \frac{\beta_2}{r\alpha} + \frac{\beta_2}{2} + \frac{2}{3}\beta_1\alpha^2r^2 - \frac{\beta_2\alpha r}{6} + \frac{\beta_3}{r^2\alpha^2} + \frac{\beta_2}{24}\alpha^2r^2 \tag{32}$$

$$V_{eff} = \left[\frac{2}{3}\beta_1 + \frac{\beta_2}{24}\right]\alpha^2r^2 + \left[-\frac{4}{3}\beta_1 - \frac{\beta_2}{6}\right]\alpha r - \frac{[2\beta_1+\beta_2]}{r\alpha} + \frac{[\beta_1+\beta_2+\beta_3]}{\alpha^2r^2} + \left[2\beta_1 + \frac{\beta_2}{2}\right] \tag{33}$$

$$V_{eff} = C_1r^2 + C_2r - \frac{C_3}{r} + \frac{C_4}{r^2} + C_5 \tag{34}$$

where,

$$C_1 = \left[\frac{2}{3}\beta_1 + \frac{\beta_2}{24}\right]\alpha^2 \tag{35}$$

$$C_2 = \left[-\frac{4}{3}\beta_1 - \frac{\beta_2}{6}\right]\alpha \tag{36}$$

$$C_3 = \frac{2\beta_1+\beta_2}{\alpha} \tag{37}$$

$$C_4 = \frac{\beta_1 + \beta_2 + \beta_3}{\alpha^2} = C(C+1) \tag{38}$$

where

$$C = -\frac{1}{2} + \sqrt{\frac{\beta_1^2 + \beta_2^2 + \beta_3^2}{\alpha^2} + \frac{1}{4}} \tag{39}$$

$$C_5 = 2\beta_1 + \frac{\beta_2}{2} \tag{40}$$

$$\frac{d^2 u_{nm}(r)}{dr^2} + \frac{2}{r}\frac{d u_{nm}(r)}{dr} + \left[\varepsilon - C_1 r^2 - C_2 r + \frac{C_3}{r} - \frac{C(C+1)}{r^2}\right] u_{nm}(r) = 0 \tag{41}$$

where $\varepsilon = -(E_{nl}^{'} + C_5)$ Now make an anzats wave function [36, 54]

$$u_{nm}(r) = e^{-\alpha r^2 - \beta r} G(r) \tag{42}$$

where α and β are positive constants. Using this wave function on Eq.(41), it becomes

$$G^{''}(r) + \left[\left(-4\alpha - 2\beta + \frac{2}{r}\right)\right] G^{'}(r) + \left[\left(4\alpha^2 r - C_1\right) r^2 + (4\alpha\beta - C_2)\, r + \frac{(C_3 - 2\beta)}{r} - \frac{C(C+1)}{r^2} + \left(\varepsilon - 6\alpha + \beta^2\right)\right] G(r) = 0 \tag{43}$$

Due to singularities in Eq. (43), the factorization wave function of the form [36, 54, 55]

$$G(r) = \sum_{n=0}^{\infty} b_n r^{2n+C} \tag{44}$$

is considered suitable to solve Eq. (43). Taking the first and second derivatives of Eq. (44) and substitute alongside with Eq. (44) into our Eq. (43), we obtain

$$\sum_{n=0}^{\infty} b_n \left[(2n + C)(2n + C - 1) + 2(2n + C) - C(C + 1)\right] r^{2n+C-2} + \left[-2\beta\,(2n + C + 1) + C_3\right] r^{2n+C-1} + \left[-4\alpha\,(2n + C) + \varepsilon + \beta^2 - 6\alpha\right] r^{2n+C} + (4\alpha\beta - C_2)\, r^{2n+C+1} + \left(4\alpha^2 - C_1\right) r^{2n+C+2} = 0 \tag{45}$$

Given that r is a non-zero function, each of the terms in equation (45) is independently equal to zero. With this in mind, we may get the following relationships for

each of the terms.

$$(2n+1)(2n+C+1)-C-C^2=0 \tag{46}$$

$$\varepsilon = 2\alpha(2n+2C+3)-\beta^2 \tag{47}$$

$$C_3 = 2\beta(2n+C+1) \tag{48}$$

$$\beta = \frac{C_2}{4\alpha} \tag{49}$$

$$C_1 = 4\alpha^2 \tag{50}$$

$$\alpha = \frac{\sqrt{C_1}}{2} \tag{51}$$

Equations (47), (48), and (51) are used to obtain the energy eigenvalue expression.

$$-(E_{nl}^{'}+C_5) = \sqrt{C_1}(2n+2C+3) - \frac{C_3^2}{4}(2n+C+1) \tag{52}$$

$$\mu_1(E_{nl}-a-D_e) = \sqrt{\left[\frac{2}{3}\mu_1(\alpha^2 a_1+\alpha a_2)+\vec{B}^2 q'^2+\frac{\mu_1\alpha(A_1-a_2)+2\alpha q_1(m+\eta)}{24}\right]\alpha^2}$$
$$\left(4n+2+2\sqrt{\frac{1}{4}+\frac{\mu_1(\alpha^2 a_1+\alpha a_2)+\mu_1\alpha(A_1-a_2)+2\alpha q_1(m+\eta)+\alpha^2\left(m'^2-\frac{1}{4}\right)+\mu_1\alpha(\alpha A_2-A_1)}{\alpha^2}}\right)-$$
$$\frac{\left(2\mu_1(\alpha^2 a_1+\alpha a_2)+\beta_2\right)^2}{4\alpha^2}$$
$$\left(4n+1+2\sqrt{\frac{1}{4}+\frac{\mu_1(\alpha^2 a_1+\alpha a_2)+\mu_1\alpha(A_1-a_2)+2\alpha q_1(m+\eta)+\alpha^2\left(m'^2-\frac{1}{4}\right)+\mu_1\alpha(\alpha A_2-A_1)}{\alpha^2}}\right)^{-2}+$$
$$2\mu_1(\alpha^2 a_1+\alpha a_2)+\frac{\mu_1\alpha(A_1-a_2)+2\alpha q_1(m+\eta)}{2} \tag{53}$$

$$E_{nl} = a+D_e+\frac{\hbar^2}{2\mu}\sqrt{\left[\frac{2}{3}\beta_1+\frac{\beta_2}{24}\right]\alpha^2}(4n+2+2\Omega)-$$
$$\frac{\hbar^2}{2\mu}\frac{(2\beta_1+\beta_2)^2}{4\alpha^2}(4n+1+2\Omega)^{-2}+\frac{\hbar^2}{2\mu}\left(2\beta_1+\frac{\beta_2}{2}\right) \tag{54}$$

The mass spectra of heavy quarkonium systems such as charmonium and bottomonium, which have the same flavour quark and antiqurak, are also obtained from the energy eigenvalue. The following equation is used to calculate the mass spectra.

$$M = m_1+m_2+E_{nl} \tag{55}$$

but,

$$m_1 = m_2 = m_b \tag{56}$$

Resulting in the expression

$$M = 2m+E_{nl} \tag{57}$$

where m_b is the mass of the particle under investigation and E_{nl} is the derived energy eigenvalues.

Substituting Eqs. (54) into (57) we obtain

$$M = 2m + a + D_e + \frac{\hbar^2}{2\mu}\sqrt{\left[\frac{2}{3}\beta_1 + \frac{\beta_2}{24}\right]\alpha^2}\,(4n + 2 + 2\Omega) - \frac{\hbar^2}{2\mu}\frac{(2\beta_1 + \beta_2)^2}{4\alpha^2}(4n + 1 + 2\Omega)^{-2} + \frac{\hbar^2}{2\mu}\left(2\beta_1 + \frac{\beta_2}{2}\right) \tag{58}$$

4.1 Special cases with an external fields

4.1.1 Generalized Kratzer potential (GKP)

Setting $a_1 = a_2 = 0$, Eq. (1) reduce into generalized Kratzer potential as [35]

$$V^{GKP}(r) = a + D_e - \left(\frac{A_1}{r} - \frac{A_2}{r^2}\right) \tag{59}$$

Energy eigenvalues corresponds to Eq. (59) with an external fields

$$E_{nm}^{GKP} = a + D_e + \frac{\hbar^2\alpha^2}{2\mu}\left(m'^2 - \frac{1}{4}\right) + \alpha^2 A_2 - \alpha A_1 - \frac{\hbar^2\alpha^2}{2\mu} \times \left[\frac{\frac{2\mu}{\hbar^2\alpha^2}\left(\alpha^2 A_2 - \alpha A_1\right) - \frac{q^2}{\hbar^2c^2\alpha^2}\vec{B}^2 + m'^2 - \frac{1}{4}}{2(n + \Omega^{GKP})} + \frac{(n + \Omega^{GKP})}{2}\right]^2 \tag{60}$$

where

$$\Omega^{GKP} = \frac{1}{2} + \sqrt{\frac{2\mu A_2}{\hbar^2} + \frac{q^2}{\hbar^2c^2\alpha^2}\vec{B}^2 + \frac{q}{\hbar c\alpha}2\vec{B}m' + m'^2} = \frac{1}{2} \tag{61}$$

4.1.2 Modified Kratzer potential

Setting $a = a_1 = a_2 = 0$, Eq. (1) convert into modified Kratzer potential as [35]

$$V^{MKP}(r) = D_e\left(\frac{r - r_e}{r}\right)^2 \tag{62}$$

Energy eigenvalues corresponds to Eqs. (62) from (22)

$$E_{nm}^{MKP} = D_e + \frac{\hbar^2\alpha^2}{2\mu}\left(m'^2 - \frac{1}{4}\right) + \alpha^2 D_e r_e^2 - 2\alpha D_e r_e - \frac{\hbar^2\alpha^2}{2\mu}$$

$$\times \left[\frac{\frac{2\mu D_e}{\hbar^2\alpha}\left(\alpha r_e^2 - 2r_e\right) - \frac{q^2}{\hbar^2 c^2\alpha^2}\vec{B}^2 + m'^2 - \frac{1}{4}}{2(n+\Omega^{MKP})} + \frac{(n+\Omega^{MKP})}{2} \right]^2 \tag{63}$$

where

$$\Omega^{MKP} = \frac{1}{2} + \sqrt{\frac{\mu D_e r_e^2}{\hbar^2} + \frac{q^2}{\hbar^2 c^2\alpha^2}\vec{B}^2 + \frac{q}{\hbar c\alpha}2\vec{B}m' + m'^2} \tag{64}$$

4.1.3 Kratzer potential

Setting $a_1 = a_2 = 0$ and $a = -D_e$, Eq. (1) convert into Kratzer potential as [35]

$$V^{KP}(r) = -2D_e\left(\frac{r_e}{r} - \frac{r_e^2}{2r^2}\right) \tag{65}$$

Energy eigenvalues corresponds to Eqs. (65) from (22)

$$E_{nm}^{KP} = \frac{\hbar^2\alpha^2}{2\mu}\left(m'^2 - \frac{1}{4}\right) + \alpha^2 D_e r_e^2 - 2\alpha D_e r_e - \frac{\hbar^2\alpha^2}{2\mu} \times \left[\frac{\frac{2\mu}{\hbar^2\alpha^2}\left(\alpha^2 D_e r_e^2 - 2\alpha D_e r_e\right) - \frac{q^2}{\hbar^2 c^2\alpha^2}\vec{B}^2 + m'^2 - \frac{1}{4}}{2(n+\Omega^{KP})} + \frac{(n+\Omega^{KP})}{2} \right]^2 \tag{66}$$

where

$$\Omega^{KP} = \frac{1}{2} + \sqrt{\frac{\mu D_e r_e^2}{\hbar^2} + \frac{q^2}{\hbar^2 c^2\alpha^2}\vec{B}^2 + \frac{q}{\hbar c\alpha}2\vec{B}m' + m'^2} \tag{67}$$

4.1.4 Hellmann potential

For $a = -D_e$, $a_2 = -a_2$ and $a_1 = A_2 = 0$, Eq. (1) covert into the Hellmann potential as [56–61]

$$V^{HP}(r) = -\frac{A_1}{r} + \frac{a_2 e^{-\alpha r}}{r} \tag{68}$$

Energy eigenvalues corresponds to Eq. (22) with an external fields

$$E_{nm}^{HP} = \frac{\hbar^2\alpha^2}{2\mu}\left(m'^2 - \frac{1}{4}\right) - \alpha A_1 - \frac{\hbar^2\alpha^2}{2\mu}$$

$$\left[\frac{\frac{2\mu}{\hbar^2\alpha}(a_2-A_1)-\frac{q^2}{\hbar^2c^2\alpha^2}\vec{B}^2+\left(m'^2-\frac{1}{4}\right)}{2(n+\Omega^{HP})}+\frac{(n+\Omega^{HP})}{2}\right]^2 \tag{69}$$

where

$$\Omega^{HP}=\frac{1}{2}+\sqrt{\frac{q^2}{\hbar^2c^2\alpha^2}\vec{B}^2+\frac{q}{\hbar c\alpha}2\vec{B}m'+m'^2} \tag{70}$$

4.2 The thermodynamic properties of the MYKP with an external fields

From the energy eigenvalues of the MYKP under influence of an external fields, we obtain the partition function $Z(\vec{B},\Phi_{AB},\beta)$ under the influence of an external fields. From partition function of the given system, we calculate mean energy $U(\vec{B},\Phi_{AB},\beta)$, mean free energy $F(\vec{B},\Phi_{AB},\beta)$, entropy $S(\vec{B},\Phi_{AB},\beta)$, specific heat capacity $C_s(\vec{B},\Phi_{AB},\beta)$, magnetization at finite temperature $(\vec{B},\Phi_{AB},\beta)$ and magnetic susceptibility $\chi_m(\vec{B},\Phi_{AB},\beta)$ at finite temperature [29] in this subsection.
Energy eigenvalues Eq. (22) reads

$$E_{nm}=L_1-\frac{\hbar^2\alpha^2}{2\mu}\left[\frac{L_2}{2(n+\Omega)}-\frac{(n+\Omega)}{2}\right]^2 \tag{71}$$

$$\begin{aligned}L_1 &= a+D_e+\frac{\hbar^2\alpha^2}{2\mu}\left(m'^2-\frac{1}{4}\right)+\alpha^2A_2-\alpha A_1\\ L_2 &= \frac{2\mu}{\hbar^2}\left(A_2-a_1-\frac{\alpha A_1-a_2}{\alpha}\right)-\frac{q^2}{\hbar^2c^2\alpha^2}\vec{B}^2+m'^2-\frac{1}{4}\end{aligned} \tag{72}$$

Exact partition function at temperature T written as [62–64]

$$Z(\vec{B},\Phi_{AB},\beta)=\sum_{\upsilon=0}^{\upsilon_{max}}e^{-\beta E_{nm}} \tag{73}$$

where $\beta=\frac{1}{kT}$, k- constant of Boltzmann and E_{nm} is the energy of the n^{th} state. From Eqs. (71) and (73) becomes

$$Z(\vec{B},\Phi_{AB},\beta)=\sum_{n=0}^{\upsilon_m}e^{-\beta\left(L_1-\frac{\hbar^2\alpha^2}{2\mu}\left[\frac{L_2}{2(n+\Omega)}-\frac{(n+\Omega)}{2}\right]^2\right)} \tag{74}$$

where

$$\upsilon_m=-\Omega\pm\sqrt{L_2} \tag{75}$$

In the classical limit, replacing the sum of Eq. (74) by an integral as [65]

$$Z(\vec{B}, \Phi_{AB}, \beta) = \int_0^{v_m} e^{\beta\left(P_1\rho^2 + \frac{P_2}{\rho^2} + P_3\right)} d\rho, \quad \rho = n + \Omega \tag{76}$$

where

$$P_1 = \frac{\hbar^2\alpha^2}{8\mu}; \quad Q_2 = \frac{\hbar^2\alpha^2}{8\mu}L_2^2; \quad P_3 = -\left(\frac{\hbar^2\alpha^2}{4\mu}L_2 + L_1\right) \tag{77}$$

Employing a Maple software, we obtain $Z(\vec{B}, \Phi_{AB}, \beta)$ as [66]

$$\begin{aligned} Z(\vec{B}, \Phi_{AB}, \beta) &= \frac{1}{2}e^{\beta(P_1\rho^2 + P_3)}\sqrt{P_2\beta} \\ &\times \left(\frac{2v_m e^{\frac{P_2\beta}{v_m^2}}}{\sqrt{P_2\beta}} - \frac{2\sqrt{\pi\, P_2\beta}\ \mathrm{erf}i\left(\frac{\sqrt{P_2\beta}}{v_m}\right)}{\sqrt{P_2\beta}} - 2\sqrt{\pi}\right) \end{aligned} \tag{78}$$

where imaginary error function erf$i$ defined as [67]

$$\mathrm{erf}i\,(x) = -i\ \mathrm{erf}(ix) = \frac{2}{\sqrt{\pi}}\int_0^x e^{t^2} dt. \tag{79}$$

Below mentioned thermodynamic and magnetic properties under influence of an external fields can be investigate using partition function [66] ,

- Mean energy

$$U(\vec{B}, \Phi_{AB}, \beta) = -\frac{\partial}{\partial(\beta)}\ln Z(\vec{B}, \Phi_{AB}, \beta) \tag{80}$$

- Mean free energy

$$F(\vec{B}, \Phi_{AB}, \beta) = -kT\ \ln Z(\vec{B}, \Phi_{AB}, \beta) \tag{81}$$

- Entropy

$$\begin{aligned} S(\vec{B}, \Phi_{AB}, \beta) &= k\ln Z(\vec{B}, \Phi_{AB}, \beta') + kT\frac{\partial}{\partial T}\ln Z(\vec{B}, \Phi_{AB}, \beta) \\ &= k\ln Z(\vec{B}, \Phi_{AB}, \beta) - k\beta\frac{\partial}{\partial\beta}\ln Z(\vec{B}, \Phi_{AB}, \beta) \end{aligned} \tag{82}$$

Table 1 Spectroscopic parameters for few selected diatomic molecules

Molecules	$D_e(eV)$	μ(a.m.u)	r_e(Å)	r_e(Å^{-1})
N_2	11.9382	7.00335	1.0940	0.000655
CH	3.947419	0.929931	1.1198	0.000885
ScH	2.25000	0.986040	1.776	1.41113
H_2	4.7446	0.50391	0.7416	1.440558

- Specific heat capacity

$$C_s(\vec{B}, \Phi_{AB}, \beta) = \frac{\partial U(\vec{B}, \Phi_{AB}, \beta)}{\partial T} = -k\beta^2 \frac{\partial U(\vec{B}, \Phi_{AB}, \beta')}{\partial \beta} = k\beta^2 \frac{\partial^2}{\partial \beta^2} \ln Z(\beta) \tag{83}$$

- Magnetization at finite temperature is written as [29, 47]

$$M(\vec{B}, \Phi_{AB}, \beta) = \frac{1}{\beta Z(\vec{B}, \Phi_{AB}, \beta)} \frac{\partial Z(\vec{B}, \Phi_{AB}, \beta)}{\partial \vec{B}} \tag{84}$$

- Magnetic susceptibility at finite temperature is written as [29, 47]

$$\chi_m(\vec{B}, \Phi_{AB}, \beta) = \frac{\partial M(\vec{B}, \Phi_{AB}, \beta)}{\partial \vec{B}} \tag{85}$$

5 Results and discussion

In Table 2, we calculates energy spectrum of the MYKP under effect of the magnetic field and AB flux field for the various values of the n and m quantum numbers with constant values of the other parameters. We tabulate numerical results for $\vec{B} = 0, 2, 4, 6, 8$ and also for $\Phi_{AB} = 2, 4, 6, 8$. At values of $\vec{B}$ and Φ_{AB} equal to zero, degeneracy is present. Energy eigenvalues decreases with increases $\vec{B}$ and magnetic quantum number m whereas it is increase with increase Φ_{AB}. Tables 3 and 4 show the energy spectrum for N_2 molecules for Kratzer potential, with different quantum numbers n, m for comparison with numerical results in NU and series expansion methods. Tables 5 and 6 show the similar methodology for CH molecules. Numerical results are compared with numerical results presented in Ref. [35]. In Table 7, we presented Numerical results of energy eigenspectrum for Hellmann potential under effect of an external fields. We tabulates numerical results for ScH and H_2 molecules for modified Kratzer potential in Tables 8 and 9. respectively. In Tables 10 and 11. we presents numerical results of the ScH and H_2 molecules for generalized Kratzer potential. Tabulated results are compared with numerical results presented in Ref. [47]. To calculates,

Table 2 Energy eigenvalues spectrum of the MYKP for the different n, m quantum numbers with constant values of the parameters $a = c = q = \hbar = \mu = 1$, $a_1 = a_2 = -1$, $A_1 = 2$, $A_2 = 4$, $D_e = 1.5$, $\alpha = 0.1$

n	m	$\vec{B} = 0, \Phi_{AB} = 0$	$\vec{B} = 2, \Phi_{AB} = 0$	$\vec{B} = 4, \Phi_{AB} = 0$	$\vec{B} = 6, \Phi_{AB} = 0$	$\vec{B} = 8, \Phi_{AB} = 0$
0	0	2.33432328	2.33831728	2.33796886	2.33782631	2.33774992
1	−1	2.33262256	2.33321836	2.33291164	2.33278679	2.33271983
	0	2.33860428	2.33084347	2.32931443	2.32874307	2.32844508
	1	2.34262256	2.31964673	2.31637827	2.31515844	2.31452194
2	−1	2.32548866	2.32545612	2.32412280	2.32361604	2.32335014
	0	2.33339177	2.31499009	2.31161221	2.31033051	2.30965739
	1	2.33548866	2.29626923	2.29013627	2.28777804	2.28653189
3	−1	2.31385196	2.30935110	2.30629547	2.30512014	2.30449994
	0	2.32295845	2.29173025	2.28545628	2.28301509	2.28171920
	1	2.32385196	2.26628005	2.25597461	2.25189148	2.24970599
n	m	$\Phi_{AB} = 0, \vec{B} = 0$	$\Phi_{AB} = 2, \vec{B} = 0$	$\Phi_{AB} = 4, \vec{B} = 0$	$\Phi_{AB} = 6, \vec{B} = 0$	$\Phi_{AB} = 8, \vec{B} = 0$
0	0	2.33432328	2.33632010	2.33897998	2.34191826	2.34464728
1	−1	2.33262256	2.33484139	2.33670650	2.33837781	2.33992677
	0	2.33860428	2.34013523	2.34148879	2.34251499	2.34301484
	1	2.34262256	2.34303122	2.34268625	2.34142286	2.33911997
2	−1	2.32548866	2.32867836	2.33121257	2.33316090	2.33455399
	0	2.33339177	2.33470595	2.33544129	2.33553273	2.33489163
	1	2.33548866	2.33473621	2.33314562	2.33063572	2.32714243
3	−1	2.31385196	2.31765810	2.32060710	2.32272490	2.32402278

Table 2 continued

n	m	$\Phi_{AB}=0, \vec{B}=0$	$\Phi_{AB}=2, \vec{B}=0$	$\Phi_{AB}=4, \vec{B}=0$	$\Phi_{AB}=6, \vec{B}=0$	$\Phi_{AB}=8, \vec{B}=0$
	0	2.32295845	2.32414014	2.32449323	2.32399351	2.32260753
	1	2.32385196	2.32233756	2.31989596	2.31649459	2.31210662
n	m	$\Phi_{AB}=\vec{B}=0$	$\Phi_{AB}=\vec{B}=2$	$\Phi_{AB}=\vec{B}=4$	$\Phi_{AB}=\vec{B}=6$	$\Phi_{AB}=\vec{B}=8$
0	0	2.33432328	2.33850676	2.33668379	2.33403984	2.33044548
1	−1	2.33262256	2.33340855	2.33169919	2.32913046	2.32559927
	0	2.33860428	2.32824475	2.32216229	2.31597634	2.30903755
	1	2.34262256	2.31420516	2.30325601	2.29326016	2.28281121
2	−1	2.32548866	2.32300577	2.31719144	2.31112845	2.30427603
	0	2.33339177	2.30993754	2.29898173	2.28899440	2.27856960
	1	2.33548866	2.28854272	2.27176161	2.25756086	2.24340496
3	−1	2.31385196	2.30457514	2.29402364	2.28420510	2.27388976
	0	2.32295845	2.28449107	2.26769301	2.25348894	2.23934920
	1	2.32385196	2.25649563	2.23266329	2.21371187	2.19554248

Table 3 Energy eigenvalues spectrum of the Kratzer potential for N_2 molecule with different n, m quantum numbers for $q = 1$

n	m	$\vec{B}=0, \eta=0$ Present	[35]	$\vec{B}=1, \eta=0$ Present	[35]	$\vec{B}=2, \eta=0$ Present	[35]	$\vec{B}=3, \eta=0$ Present	[35]
0	0	− 11.88386399	− 11.88381894	− 11.88371596	− 11.88371512	− 11.88327187	-11.88361129	− 11.88253181	− 11.88350747
1	− 1	− 11.77605540	− 11.77593347	− 11.77628712	− 11.77582965	− 11.77622679	− 11.77572582	− 11.77587442	− 11.77562200
	0	− 11.77629970	− 11.77617777	− 11.77615367	− 11.77607347	− 11.77571561	− 11.77596918	− 11.77498557	− 11.77561916
	1	− 11.77605540	− 11.77593347	− 11.77553165	− 11.77582965	− 11.77471596	− 11.77572582	− 11.77360845	− 11.77562200
2	− 1	− 11.66994925	− 11.66975149	− 11.67017785	− 11.66964719	− 11.67011834	− 11.66954290	− 11.66977072	− 11.66943860
	0	− 11.67019025	− 11.66999248	− 11.67004620	− 11.66988771	− 11.66961405	− 11.66978294	− 11.66889387	− 11.66967818
	1	− 11.66994925	− 11.66975149	− 11.66943257	− 11.66964719	− 11.66862789	− 11.66954290	− 11.66753533	− 11.66943860
3	− 1	− 11.56527178	− 11.56499920	− 11.56549731	− 11.56489443	− 11.56543859	− 11.56478966	− 11.56509565	− 11.56468489
	0	− 11.56550954	− 11.56523696	− 11.56536742	− 11.5613172	− 11.56494108	− 11.56502648	− 11.56423058	− 11.56492124
	1	− 11.56527178	− 11.56499920	− 11.56476204	− 11.56489443	− 11.56396817	− 11.56478966	− 11.56289029	− 11.56468489
n	*m*	$\vec{B}=0, \eta=0$ Present	[35]	$\vec{B}=0, \eta=1$ Present	[35]	$\vec{B}=0, \eta=2$ Present	[35]	$\vec{B}=0, \eta=3$ Present	[35]
0	0	− 11.88386399	− 11.88381894	− 11.88361634	− 11.88357129	− 11.88287343	− 11.88282838	− 11.88163545	− 11.88159041
1	− 1	− 11.77605540	− 11.77593347	− 11.77629970	− 11.77617777	− 11.77605540	− 11.77593347	− 11.77532255	− 11.77520064
	0	− 11.77629970	− 11.77617777	− 11.77605540	− 11.77593347	− 11.77532255	− 11.77520064	− 11.77410136	− 11.77397945
	1	− 11.77605540	− 11.77593347	− 11.77532255	− 11.77520064	− 11.77410136	− 11.77397954	− 11.77239210	− 11.77227022
2	− 1	− 11.66994925	− 11.66975149	− 11.67019025	− 11.66999248	− 11.66994925	− 11.66975149	− 11.66922629	− 11.66902854
	0	− 11.67019025	− 11.66999248	− 11.66994925	− 11.66975149	− 11.66922629	− 11.66902854	− 11.66802157	− 11.66782383
	1	− 11.66994925	− 11.66975149	− 11.66922629	− 11.66902854	− 11.66802157	− 11.66782383	− 11.66633537	− 11.66613766
3	− 1	− 11.56527178	− 11.56499920	− 11.56550954	− 11.56523696	− 11.56527178	− 11.56499920	− 11.56455853	− 11.56428596
	0	− 11.56550954	− 11.56523696	− 11.56527178	− 11.56499920	− 11.56455853	− 11.56428596	− 11.56336999	− 11.56309744
	1	− 11.56527178	− 11.56499920	− 11.56455853	− 11.56428596	− 11.56336999	− 11.56309744	− 11.56170644	− 11.56143392

Table 4 Energy eigenvalues spectrum of the Kratzer potential for N_2 molecule with different n, m quantum numbers for $q = 1$ and comparison with numerical results in NU method and Series expansion method

n	m	$\vec{B} = 0, \eta = 0$ NU	SEM	$\vec{B} = 1, \eta = 0$ NU	SEM	$\vec{B} = 2, \eta = 0$ NU	SEM	$\vec{B} = 3, \eta = 0$ NU	SEM
0	0	− 11.88386399	− 11.88386399	− 11.88371596	− 11.88371596	− 11.88327187	− 11.88327187	− 11.88253181	− 11.88253181
1	− 1	− 11.77605540	− 11.77605540	− 11.77628712	− 11.77628712	− 11.77622679	− 11.77622679	− 11.77587442	− 11.77587442
	0	− 11.77629970	− 11.77629970	− 11.77615367	− 11.77615367	− 11.77571561	− 11.77571561	− 11.77498557	− 11.77498557
	1	− 11.77605540	− 11.77605540	− 11.77553165	− 11.77553165	− 11.77471596	− 11.77471596	− 11.77360845	− 11.77360845
2	− 1	− 11.66994925	− 11.66994925	− 11.67017785	− 11.67017785	− 11.67011834	− 11.67011834	− 11.66977072	− 11.66977072
	0	− 11.67019025	− 11.67019025	− 11.67004620	− 11.67004620	− 11.66961405	− 11.66961405	− 11.66889387	− 11.66889387
	1	− 11.66994925	− 11.66994925	− 11.66943257	− 11.66943257	− 11.66862789	− 11.66862789	− 11.66753533	− 11.66753533
3	− 1	− 11.56527178	− 11.56527178	− 11.56549731	− 11.56549731	− 11.56543859	− 11.56543859	− 11.56509565	− 11.56509565
	0	− 11.56550954	− 11.56550954	− 11.56536742	− 11.56536742	− 11.56494108	− 11.56494108	− 11.56423058	− 11.56423058
	1	− 11.56527178	− 11.56527178	− 11.56476204	− 11.56476204	− 11.56396817	− 11.56396817	− 11.56289029	− 11.56289029
n	m	$\vec{B} = 0, \eta = 0$ NU	SEM	$\vec{B} = 0, \eta = 1$ NU	SEM	$\vec{B} = 0, \eta = 2$ NU	SEM	$\vec{B} = 0, \eta = 3$ NU	SEM
0	0	− 11.88386399	− 11.88386399	− 11.88361634	− 11.88361634	− 11.88287343	− 11.88287343	− 11.88163545	− 11.88163545
1	− 1	− 11.77605540	− 11.77605540	− 11.77629970	− 11.77629970	− 11.77605540	− 11.77605540	− 11.77532255	− 11.77532255
	0	− 11.77629970	− 11.77629970	− 11.77605540	− 11.77605540	− 11.77532255	− 11.77532255	− 11.77410136	− 11.77410136
	1	− 11.77605540	− 11.77605540	− 11.77532255	− 11.77532255	− 11.77410136	− 11.77410136	− 11.77239210	− 11.77239210
2	− 1	− 11.66994925	11.66994925	− 11.67019025	− 11.67019025	− 11.66994925	− 11.66994925	− 11.66922629	− 11.66922629
	0	− 11.67019025	− 11.67019025	− 11.66994925	− 11.66994925	− 11.66922629	− 11.66922629	− 11.66802157	− 11.66802157
	1	− 11.66994925	− 11.66994925	− 11.66922629	− 11.66922629	− 11.66802157	− 11.66802157	− 11.66633537	− 11.66633537
3	− 1	− 11.56527178	− 11.56527178	− 11.56550954	− 11.56550954	− 11.56527178	− 11.56527178	− 11.56455853	− 11.56455853
	0	− 11.56550954	− 11.56550954	− 11.56527178	− 11.56527178	− 11.56455853	− 11.56455853	− 11.56336999	− 11.56336999
	1	− 11.56527178	− 11.56527178	− 11.56455853	− 11.56455853	− 11.56336999	− 11.56336999	− 11.56170644	− 11.56170644

Table 5 Energy eigenvalues spectrum of the Kratzer potential for CH molecule with different n, m quantum numbers for $q = 1$

n	m	$\vec{B}=0,\eta=0$ Present	[35]	$\vec{B}=1,\eta=0$ Present	[35]	$\vec{B}=2,\eta=0$ Present	[35]	$\vec{B}=3,\eta=0$ Present	[35]
0	0	− 3.86471115	− 3.86462852	− 3.86414303	− 3.86445802	− 3.86243970	− 3.41686928	− 3.85960416	− 3.86411704
1	− 1	− 3.70528338	− 3.70504461	− 3.70661498	− 3.70487408	− 3.70687984	− 3.70470355	− 3.70607749	− 3.70453302
	0	− 3.70691369	− 3.70667486	− 3.70638005	− 3.70650081	− 3.70478009	− 3.70632676	− 3.70211657	− 3.70615271
	1	− 3.70528338	− 3.70504461	− 3.70288735	− 3.70486696	− 3.69943107	− 3.70468932	− 3.69492052	− 3.70451167
2	− 1	− 3.55706296	− 3.55667739	− 3.55831539	− 3.55650330	− 3.55856452	− 3.55632921	− 3.55780994	− 3.55615512
	0	− 3.55859635	− 3.55821069	− 3.55809447	− 3.55803309	− 3.55658967	− 3.55785548	− 3.55408455	− 3.55767787
	1	− 3.55706296	− 3.55667739	− 3.55480939	− 3.55649619	− 3.55155855	− 3.55631498	− 3.54731598	− 3.55613378
3	− 1	− 3.41757067	− 3.41704692	− 3.41875008	− 3.41686928	− 3.41898472	− 3.41669163	− 3.41827419	− 3.41651398
	0	− 3.41901468	− 3.41849082	− 3.41854207	− 3.41830965	− 3.41712505	− 3.41812848	− 3.41476601	− 3.41794732
	1	− 3.41757067	− 3.41704692	− 3.41544849	− 3.41686216	− 3.41238712	− 3.41667740	− 3.40839172	− 3.41649264
n	m	$\vec{B}=0,\eta=0$ Present	[35]	$\vec{B}=0,\eta=1$ Present	[35]	$\vec{B}=0,\eta=2$ Present	[35]	$\vec{B}=0,\eta=3$ Present	[35]
0	0	− 3.86471115	− 3.86462852	− 3.86297557	− 3.86289297	− 3.85777822	− 3.85769569	− 3.84914706	− 3.84906466
1	− 1	− 3.70528338	− 3.70504461	− 3.70691369	− 3.70667486	− 3.70528338	− 3.70504461	− 3.70040111	− 3.70016252
	0	− 3.70691369	− 3.70667486	− 3.70528338	− 3.70504461	− 3.70040111	− 3.70016252	− 3.69229276	− 3.69205445
	1	− 3.70528338	− 3.70504461	− 3.70040111	− 3.70016252	− 3.69229276	− 3.69205445	− 3.68100105	− 3.68076315
2	− 1	− 3.55706296	− 3.55667739	− 3.55859635	− 3.55821069	− 3.55706296	− 3.55667739	− 3.55247081	− 3.55208550
	0	− 3.55859635	− 3.55821069	− 3.55706296	− 3.55667739	− 3.55247081	− 3.55208550	− 3.54484387	− 3.54445900
	1	− 3.55706296	− 3.55667739	− 3.55247081	− 3.55208550	− 3.54484387	− 3.54445900	− 3.53422174	− 3.53383747
3	− 1	− 3.41757067	− 3.41704692	− 3.41901468	− 3.41849082	− 3.41757067	− 3.41704692	− 3.41324610	− 3.41272269
	0	− 3.41901468	− 3.41849082	− 3.41757067	− 3.41272269	− 3.41324610	− 3.41272269	− 3.40606321	− 3.40554035
	1	− 3.41757067	− 3.41704692	− 3.41324610	− 3.41704692	− 3.40606321	− 3.40554035	− 3.39605873	− 3.39553666

Table 6 Energy eigenvalues spectrum of the Kratzer potential for CH molecule with different n, m quantum numbers for $q = 1$ and comparison with numerical results in NU method and Series expansion method

n	m	$\vec{B} = 0, \eta = 0$ NU	SEM	$\vec{B} = 1, \eta = 0$ NU	SEM	$\vec{B} = 2, \eta = 0$ NU	SEM	$\vec{B} = 3, \eta = 0$ NU	SEM
0	0	− 3.86471115	− 3.86471115	− 3.86414303	− 3.86414303	− 3.86243970	− 3.86243970	− 3.85960416	− 3.85960416
1	− 1	− 3.70528338	− 3.70528338	− 3.70661498	− 3.70661498	− 3.70687984	− 3.70687984	− 3.70607749	− 3.70607749
	0	− 3.70691369	− 3.70691369	− 3.70638005	− 3.70638005	− 3.70478009	− 3.70478009	− 3.70211657	− 3.70211657
	1	− 3.70528338	− 3.70528338	− 3.70288735	− 3.70288735	− 3.69943107	− 3.69943107	− 3.69492052	− 3.69492052
2	− 1	− 3.55706296	− 3.55706296	− 3.55831539	− 3.55831539	− 3.55856452	− 3.55856452	− 3.55780994	− 3.55780994
	0	− 3.55859635	− 3.55859635	− 3.55809447	− 3.55809447	− 3.55658967	− 3.55658967	− 3.55408455	− 3.55408455
	1	− 3.55706296	− 3.55706296	− 3.55480939	− 3.55480939	− 3.55155855	− 3.55155855	− 3.54731598	− 3.54731598
3	− 1	− 3.41757067	− 3.41757067	− 3.41875008	− 3.41875008	− 3.41898472	− 3.41898472	− 3.41827419	− 3.41827419
	0	− 3.41901468	− 3.41901468	− 3.41854207	− 3.41854207	− 3.41712505	− 3.41712505	− 3.41476601	− 3.41476601
	1	− 3.41757067	− 3.41757067	− 3.41544849	− 3.41544849	− 3.41238712	− 3.41238712	− 3.40839172	− 3.40839172
n	m	$\vec{B} = 0, \eta = 0$ NU	SEM	$\vec{B} = 0, \eta = 1$ NU	SEM	$\vec{B} = 0, \eta = 2$ NU	SEM	$\vec{B} = 0, \eta = 3$ NU	SEM
0	0	− 3.86471115	− 3.86471115	− 3.86297557	− 3.86297557	− 3.85777822	− 3.85777822	− 3.84914706	− 3.84914706
1	− 1	− 3.70528338	− 3.70528338	-3.70691369	− 3.70691369	− 3.70528338	− 3.70528338	− 3.70040111	− 3.70040111
	0	− 3.70691369	− 3.70691369	− 3.70528338	− 3.70528338	− 3.70040111	− 3.70040111	− 3.69229276	− 3.69229276
	1	− 3.70528338	− 3.70528338	− 3.70040111	− 3.70040111	− 3.69229276	− 3.69229276	− 3.68100105	− 3.68100105
2	− 1	− 3.55706296	− 3.55706296	− 3.55859635	− 3.55859635	− 3.55706296	− 3.55706296	− 3.55247081	− 3.55247081
	0	− 3.55859635	− 3.55859635	− 3.55706296	− 3.55706296	− 3.55247081	− 3.55247081	− 3.54484387	− 3.54484387
	1	− 3.55706296	− 3.55706296	− 3.55247081	− 3.55247081	− 3.54484387	− 3.54484387	− 3.53422174	− 3.53422174
3	− 1	− 3.41757067	− 3.41757067	− 3.41901468	− 3.41901468	− 3.41757067	− 3.41757067	− 3.41324610	− 3.41324610
	0	− 3.41901468	− 3.41901468	− 3.41757067	− 3.41757067	− 3.41324610	− 3.41324610	− 3.40606321	− 3.40606321
	1	− 3.41757067	− 3.41757067	− 3.41324610	− 3.41324610	− 3.40606321	− 3.40606321	− 3.39605873	− 3.39605873

Table 7 Energy eigenvalues spectrum of the Hellmann potential with different n, m quantum numbers and various values of the magnetic field B for $\Phi_{AB} = 0$ and parameters $q = \hbar = h = c = \mu = 1$ with screening parameter $\alpha = 0.01$ and $A_1 = 0.5$, $a = -0.5$

n	m	$\vec{B} = 0$		$\vec{B} = 2$		$\vec{B} = 4$		$\vec{B} = 6$		$\vec{B} = 8$	
		Present	[47]	Present	[47]	Present	[47]	Present	[47]	Present	[47]
0	0	− 2.0050125	− 2.0050125	− 0.0050125	− 0.0050125	− 0.0050156	− 0.0050156	− 0.0050180	− 0.0050180	− 0.0050195	− 0.0050195
1	− 1	− 0.0794605	− 0.0794605	− 0.0049625	− 0.0049625	− 0.0049656	− 0.0049656	− 0.0049680	− 0.0049680	− 0.0049695	− 0.0049695
	0	− 0.2228130	− 0.2228130	− 0.0050622	− 0.0050622	− 0.0050903	− 0.0050903	− 0.0051011	− 0.0051011	− 0.0051068	− 0.0051068
	1	− 0.0794605	− 0.0794605	− 0.0051610	− 0.0051610	− 0.0052144	− 0.0052144	− 0.0052338	− 0.0052338	− 0.0052440	− 0.0052440
2	− 2	− 0.0239334	− 0.0239334	− 0.0048125	− 0.0048125	− 0.0048157	− 0.0048157	− 0.0048181	− 0.0048181	− 0.0048196	− 0.0048196
	− 1	− 0.0406451	− 0.0406451	− 0.0050125	− 0.0050125	− 0.0050405	− 0.0050405	− 0.0050512	− 0.0050512	− 0.0050569	− 0.0050569
	0	− 0.0802845	− 0.0802845	− 0.0052105	− 0.0052105	− 0.0052641	− 0.0052641	− 0.0052836	− 0.0052836	− 0.0052936	− 0.0052936
	1	− 0.0406451	− 0.0406451	− 0.0054066	− 0.0054066	− 0.0054867	− 0.0054867	− 0.0055152	− 0.0055152	− 0.0055298	− 0.0055298
	2	− 0.0239334	− 0.0239334	− 0.0056008	− 0.0056008	− 0.0057080	− 0.0057080	− 0.0057460	− 0.0057460	− 0.0057653	− 0.0057653
3	− 3	− 0.0111308	− 0.0111308	− 0.0045625	− 0.0045625	− 0.0045659	− 0.0045659	− 0.0045683	− 0.0045683	− 0.0045697	− 0.0045697
	− 2	− 0.0161992	− 0.0161992	− 0.0048632	− 0.0048632	− 0.0048909	− 0.0048909	− 0.0049016	− 0.0049016	− 0.0049071	− 0.0049071
	− 1	− 0.0247408	− 0.0247408	− 0.0051610	− 0.0051610	− 0.0052144	− 0.0052144	− 0.0052338	− 0.0052338	− 0.0052438	− 0.0052438
	0	− 0.0410778	− 0.0410778	− 0.0054559	− 0.0054559	− 0.0055363	− 0.0055363	− 0.0055649	− 0.0055649	− 0.0055795	− 0.0055795
	1	− 0.0247408	− 0.0247408	− 0.0057479	− 0.0057479	− 0.0058565	− 0.0058565	− 0.0058949	− 0.0058949	− 0.0059145	− 0.0059145
	2	− 0.0161992	− 0.0161992	− 0.0060370	− 0.0060370	− 0.0061752	− 0.0061752	− 0.0062238	− 0.0062238	− 0.0062486	− 0.0062486
	3	− 0.0111308	− 0.0111308	− 0.0063234	− 0.0063234	− 0.0064924	− 0.0064924	0.00655170	0.00655170	− 0.0065819	− 0.0065819

Table 7 continued

n	m	$\vec{B}=0$ Present	[47]	$\vec{B}=2$ Present	[47]	$\vec{B}=4$ Present	[47]	$\vec{B}=6$ Present	[47]	$\vec{B}=8$ Present	[47]
4	− 4	− 0.0063827	− 0.0063827	− 0.0042126	− 0.0042126	− 0.0042161	− 0.0042161	− 0.0042185	− 0.0042185	− 0.0042190	− 0.0042190
	− 3	− 0.0086125	− 0.0086125	− 0.0046145	− 0.0046145	− 0.0046417	− 0.0046417	− 0.0046521	− 0.0046521	− 0.0046576	− 0.0046576
	− 2	− 0.0118291	− 0.0118291	− 0.0050125	− 0.0050125	− 0.0050653	− 0.0050653	− 0.0050844	− 0.0050844	− 0.0050942	− 0.0050942
	− 1	− 0.0167645	− 0.0167645	− 0.0054066	− 0.0054066	− 0.0054867	− 0.0054867	− 0.0055152	− 0.0055152	− 0.0055298	− 0.0055298
	0	− 0.0250125	− 0.0250125	− 0.0057969	− 0.0057969	− 0.0059060	− 0.0059060	− 0.0059446	− 0.0059446	− 0.0059642	− 0.0059642
	1	− 0.0167645	− 0.0167645	− 0.0167645	− 0.0167645	− 0.0063233	− 0.0063233	− 0.0063725	− 0.0063725	− 0.0063976	− 0.0063976
	2	− 0.0118290	− 0.0118290	− 0.0065663	− 0.0065663	− 0.0067386	− 0.0067386	− 0.0067991	− 0.0067991	− 0.0068299	− 0.0068299
	3	− 0.0086125	− 0.0086125	− 0.0069455	− 0.0069455	− 0.0071518	− 0.0071518	− 0.0072243	− 0.0072243	− 0.0072612	− 0.0072612
	4	− 0.0063827	− 0.0063827	− 0.0073211	− 0.0073211	− 0.0075630	− 0.0075630	− 0.0076481	− 0.0076481	− 0.0076914	− 0.0076914

Table 8 Energy eigenvalues spectrum of the modified Kratzer potential for ScH molecule with different n, m quantum numbers and magnetic field B for $\Phi_{AB} = 0$ and $q = 1$

n	m	$\Phi_{AB} = 0, B = 0$	$\Phi_{AB} = 0, B = 2$	$\Phi_{AB} = 0, B = 4$	$\Phi_{AB} = 0, B = 6$	$\Phi_{AB} = 0, B = 8$
0	0	− 0.0220773860	− 0.0220773859	− 0.0220773856	− 0.0220773850	− 0.0220773843
1	− 1	− 0.0662691051	− 0.0662688979	− 0.0662686906	− 0.0662684830	− 0.0662682752
	0	− 0.0663632555	− 0.0663632553	− 0.0663632550	− 0.0663632545	− 0.0663632537
	1	− 0.0662691051	− 0.0662693120	− 0.0662695187	− 0.0662697252	− 0.0662699315
2	− 1	− 0.1108874292	− 0.1108872205	− 0.1108870116	− 0.1108868024	− 0.1108865931
	0	− 0.1109812530	− 0.1109812529	− 0.1109812525	− 0.1109812520	− 0.1109812512
	1	− 0.1108874292	− 0.1108876377	− 0.1108878459	− 0.1108880540	− 0.1108882618
3	− 1	− 0.1558370083	− 0.1558367981	− 0.1558365876	− 0.1558363770	− 0.1558361661
	0	− 0.1559304941	− 0.1559304940	− 0.1559304937	− 0.1559304932	− 0.1559304924
	1	− 0.1558370083	− 0.1558372183	− 0.1558374281	− 0.1558376377	− 0.1558378471
4	− 1	− 0.2011169856	− 0.2011167738	− 0.2011165618	− 0.2011163496	− 0.2011161372
	0	− 0.2012101223	− 0.2012101222	− 0.2012101219	− 0.2012101214	− 0.2012101206
	1	− 0.2011169856	− 0.2011171971	− 0.2011174085	− 0.2011176196	− 0.2011178305
5	− 1	− 0.2467265308	− 0.2467263175	− 0.2467261039	− 0.2467258902	− 0.2467256763
	0	− 0.2468193076	− 0.2468193075	− 0.2468193072	− 0.2468193067	− 0.2468193059
	1	− 0.2467265308	− 0.2467267439	− 0.2467269567	− 0.2467271694	− 0.2467273819
n	m	$\vec{B} = 0, \Phi_{AB} = 0$	$\vec{B} = 0, \Phi_{AB} = 2$	$\vec{B} = 0, \Phi_{AB} = 4$	$\vec{B} = 0, \Phi_{AB} = 6$	$\vec{B} = 0, \Phi_{AB} = 8$
0	0	− 0.0220773860	− 0.02207738606	− 0.02207738605	− 0.02207738604	− 0.02207738602
1	− 1	− 0.0662691051	− 0.0662691355	− 0.0662691658	− 0.06626919623	− 0.06626922659
	0	− 0.0663632555	− 0.0663632554	− 0.0663632554	− 0.06636325547	− 0.06636325546
	1	− 0.0662691051	− 0.0662690747	− 0.0662690443	− 0.06626901399	− 0.06626898360

Table 8 continued

n	m	$\vec{B}=0,\Phi_{AB}=0$	$\vec{B}=0,\Phi_{AB}=2$	$\vec{B}=0,\Phi_{AB}=4$	$\vec{B}=0,\Phi_{AB}=6$	$\vec{B}=0,\Phi_{AB}=8$
2	− 1	− 0.1108874292	− 0.1108874594	− 0.1108874897	− 0.11088752001	− 0.11088755026
	0	− 0.1109812530	− 0.1109812530	− 0.1109812530	− 0.11098125299	− 0.11098125297
	1	− 0.1108874292	− 0.1108873989	− 0.1108873686	− 0.11088733840	− 0.11088730811
3	− 1	− 0.1558370083	− 0.1558370385	− 0.1558370686	− 0.15583709881	− 0.15583712895
	0	− 0.1559304941	− 0.1559304942	− 0.1559304941	− 0.15593049416	− 0.15593049414
	1	− 0.1558370083	− 0.1558369782	− 0.1558369480	− 0.15583691785	− 0.15583688768
4	− 1	− 0.2011169856	− 0.2011170156	− 0.2011170456	− 0.20111707572	− 0.20111710575
	0	− 0.2012101223	− 0.2012101224	− 0.2012101224	− 0.20121012235	− 0.20121012233
	1	− 0.2011169856	− 0.2011169555	− 0.2011169255	− 0.20111689544	− 0.20111686538
5	− 1	− 0.2467265308	− 0.2467265607	− 0.2467265906	− 0.24672662057	− 0.24672665048
	0	− 0.2468193076	− 0.2468193077	− 0.2468193076	− 0.24681930764	− 0.24681930762
	1	− 0.2467265308	− 0.2467265008	− 0.2467264709	− 0.24672644099	− 0.24672641104
n	m	$\vec{B}=\Phi_{AB}=0$	$\vec{B}=\Phi_{AB}=2$	$\vec{B}=\Phi_{AB}=4$	$\vec{B}=\Phi_{AB}=6$	$\vec{B}B=\Phi_{AB}=8$
0	0	− 0.0220773860	− 0.02207738598	− 0.02207738574	− 0.02207738535	− 0.02207738479
1	− 1	− 0.0662691051	− 0.06626892839	-0.06626875148	− 0.06626857442	− 0.06626839721
	0	− 0.0663632555	− 0.06636325542	− 0.06636325518	− 0.06636325479	− 0.06636325424
	1	− 0.0662691051	− 0.06626928172	− 0.06626945816	− 0.06626963443	− 0.06626981055
2	− 1	− 0.1108874292	− 0.11088725083	− 0.11088707228	− 0.11088689357	− 0.11088671471
	0	− 0.1109812530	− 0.11098125293	− 0.11098125270	− 0.11098125232	− 0.11098125178
	1	− 0.1108874292	− 0.11088760747	− 0.11088778555	− 0.11088796349	− 0.11088814126

Table 8 continued

n	m	$\vec{B} = \Phi_{AB} = 0$	$\vec{B} = \Phi_{AB} = 2$	$\vec{B} = \Phi_{AB} = 4$	$\vec{B} = \Phi_{AB} = 6$	$\vec{B}B = \Phi_{AB} = 8$
3	− 1	− 0.1558370083	− 0.15583682831	− 0.15583664811	− 0.15583646776	− 0.15583628726
	0	− 0.1559304941	− 0.15593049411	− 0.15593049388	− 0.15593049350	− 0.15593049297
	1	− 0.1558370083	− 0.15583718824	− 0.15583736798	− 0.15583754757	− 0.15583772701
4	− 1	− 0.2011169856	− 0.20111680391	− 0.20111662207	− 0.20111644007	− 0.20111625793
	0	− 0.2012101223	− 0.20121012230	− 0.20121012207	− 0.20121012170	− 0.20121012117
	1	− 0.2011169856	− 0.20111716714	− 0.20111734854	− 0.20111752978	− 0.20111771088
5	− 1	− 0.2467265308	− 0.24672634746	− 0.24672616397	− 0.24672598034	− 0.24672579655
	0	− 0.2468193076	− 0.24681930758	− 0.24681930736	− 0.24681930700	− 0.24681930648
	1	− 0.2467265308	− 0.24672671399	− 0.24672689704	− 0.24672707994	− 0.24672726269

Table 9 Energy eigenvalues spectrum of the modified KP for H_2 molecule with different n, m quantum numbers and magnetic field $\Phi_{AB} = 0$ for various values of the $\vec{B}$ and $q = 1$

n	m	$\Phi_{AB} = 0, \vec{B} = 0$	$\Phi_{AB} = 0, \vec{B} = 2$	$\Phi_{AB} = 0, \vec{B} = 4$	$\Phi_{AB} = 0, \vec{B} = 6$	$\Phi_{AB} = 0, \vec{B} = 8$
0	0	− 0.01663513376	− 0.01663513374	− 0.01663513368	− 0.01663513357	− 0.01663513342
1	− 1	− 0.04901873681	− 0.04901745138	− 0.04901616590	− 0.04901488037	− 0.04901359479
	0	− 0.05575126519	− 0.05575126517	− 0.05575126508	− 0.05575126494	− 0.05575126475
	1	− 0.04901873681	− 0.04902002219	− 0.04902130752	− 0.04902259280	− 0.04902387803
2	− 1	− 0.10071532548	− 0.10071371783	− 0.10071211012	− 0.10071050235	− 0.10070889452
	0	− 0.10698075340	− 0.10698075337	− 0.10698075327	− 0.10698075311	− 0.10698075289
	1	− 0.10071532548	− 0.10071693308	− 0.10071854061	− 0.10072014809	− 0.10072175550
3	− 1	− 0.16340778725	− 0.16340588459	− 0.16340398186	− 0.16340207908	− 0.16340017623
	0	− 0.16925001772	− 0.16925001769	− 0.16925001759	− 0.16925001740	− 0.16925001719
	1	− 0.16340778725	− 0.16340968984	− 0.16341159238	− 0.16341349485	− 0.16341539726
4	− 1	− 0.23620730027	− 0.23620512537	− 0.23620295042	− 0.23620077540	− 0.23619860032
	0	− 0.24166381324	− 0.24166381321	− 0.24166381311	− 0.24166381295	− 0.24166381273
	1	− 0.23620730027	− 0.23620947510	− 0.23621164987	− 0.23621382458	− 0.23621599923
5	− 1	− 0.31836785165	− 0.31836542370	− 0.31836299569	− 0.31836056763	− 0.31835813950
	0	− 0.32347082806	− 0.32347082803	− 0.32347082795	− 0.32347082780	− 0.32347082760
	1	− 0.31836785165	− 0.31837027955	− 0.31837270739	− 0.31837513517	− 0.31837756290
n	m	$\vec{B} = 0, \Phi_{AB} = 0$	$\vec{B} = 0, \Phi_{AB} = 2$	$\vec{B} = 0, \Phi_{AB} = 4$	$\vec{B} = 0, \Phi_{AB} = 6$	$\vec{B} = 0, \Phi_{AB} = 8$
0	0	− 0.01663513376	− 0.01663513357	− 0.01663513301	− 0.01663513206	− 0.01663513074
1	− 1	− 0.04901873681	− 0.04902090542	− 0.04902307369	− 0.04902524161	− 0.04902740918
	0	− 0.05575126519	− 0.05575126502	− 0.05575126449	− 0.05575126362	− 0.05575126239
	1	− 0.04901873681	− 0.04901656785	− 0.04901439854	− 0.04901222888	− 0.04901005887

Table 9 continued

n	m	$\vec{B}=0, \Phi_{AB}=0$	$\vec{B}=0, \Phi_{AB}=2$	$\vec{B}=0, \Phi_{AB}=4$	$\vec{B}=0, \Phi_{AB}=6$	$\vec{B}=0, \Phi_{AB}=8$
2	− 1	− 0.10071532548	− 0.10071734375	− 0.10071936170	− 0.10072137932	− 0.10072339661
	0	− 0.10698075340	− 0.10698075323	− 0.10698075274	− 0.10698075193	− 0.10698075079
	1	− 0.10071532548	− 0.10071330689	− 0.10071128798	− 0.10070926874	− 0.10070724918
3	− 1	− 0.16340778725	− 0.16340966929	− 0.16341155102	− 0.16341343246	− 0.16341531359
	0	− 0.16925001772	− 0.16925001757	− 0.16925001711	− 0.16925001635	− 0.16925001529
	1	− 0.16340778725	− 0.16340590490	− 0.16340402226	− 0.16340213932	− 0.16340025607
4	− 1	− 0.23620730027	− 0.23620905813	− 0.23621081572	− 0.23621257302	− 0.23621433004
	0	− 0.24166381324	− 0.24166381310	− 0.24166381267	− 0.24166381196	− 0.24166381096
	1	− 0.23620730027	− 0.23620554212	− 0.23620378369	− 0.23620202498	− 0.23620026598
5	− 1	− 0.31836785165	− 0.31836949569	− 0.31837113947	− 0.31837278299	− 0.31837442624
	0	− 0.32347082806	− 0.32347082793	− 0.32347082750	− 0.32347082686	− 0.32347082593
	1	− 0.31836785165	− 0.31836620734	− 0.31836456277	− 0.31836291794	− 0.31836127284
n	m	$\vec{B}=\Phi_{AB}=0$	$\vec{B}=\Phi_{AB}=2$	$\vec{B}=\Phi_{AB}=4$	$\vec{B}=\Phi_{AB}=6$	$\vec{B}=\Phi_{AB}=8$
0	0	− 0.01663513376	− 0.01663513370	− 0.01663513351	− 0.01663513320	− 0.01663513276
1	− 1	− 0.04901873681	− 0.04901962020	− 0.04902050363	− 0.04902138707	− 0.04902227055
	0	− 0.05575126519	− 0.05575126520	− 0.05575126520	− 0.05575126521	− 0.05575126523
	1	− 0.04901873681	− 0.04901785344	− 0.04901697009	− 0.04901608677	− 0.04901520348
2	− 1	− 0.10071532548	− 0.10071573636	− 0.10071614738	− 0.10071655855	− 0.10071696986
	0	− 0.10698075340	− 0.10698075346	− 0.10698075365	− 0.10698075396	− 0.10698075440
	1	− 0.10071532548	− 0.10071491475	− 0.10071450416	− 0.10071409371	− 0.10071368340
3	− 1	− 0.16340778725	− 0.16340776694	− 0.16340774688	− 0.16340772708	− 0.16340770754
	0	− 0.16925001772	− 0.16925001784	− 0.16925001820	− 0.16925001880	− 0.16925001964
	1	− 0.16340778725	− 0.16340780781	− 0.16340782863	− 0.16340784971	− 0.16340787104

Table 9 continued

n	m	$\vec{B} = \Phi_{AB} = 0$	$\vec{B} = \Phi_{AB} = 2$	$\vec{B} = \Phi_{AB} = 4$	$\vec{B} = \Phi_{AB} = 6$	$\vec{B} = \Phi_{AB} = 8$
4	− 1	− 0.23620730027	− 0.23620688359	− 0.23620646728	− 0.23620605134	− 0.23620563575
	0	− 0.24166381324	− 0.24166381341	− 0.24166381394	− 0.24166381482	− 0.24166381604
	1	− 0.23620730027	− 0.23620771730	− 0.23620813471	− 0.23620855247	− 0.23620897060
5	− 1	− 0.31836785165	− 0.31836863563	− 0.31836628509	− 0.31836550251	− 0.31836472040
	0	− 0.32347082806	− 0.32347082829	− 0.32347082898	− 0.32347083012	− 0.32347083172
	1	− 0.31836785165	− 0.31836863563	− 0.31836942009	− 0.31837020501	− 0.31837099040

Table 10 Energy eigenvalues spectrum of the GKP for ScH molecule with different n, m quantum numbers and magnetic field $B = 0$ for various values of the Φ_{AB}.$q = 1$ with $a = -0.5$

n	m	$\Phi_{AB} = 0, \vec{B} = 0$	$\Phi_{AB} = 0, \vec{B} = 2$	$\Phi_{AB} = 0, \vec{B} = 4$	$\Phi_{AB} = 0, \vec{B} = 6$	$\Phi_{AB} = 0, \vec{B} = 8$
0	0	− 0.52207738606	− 0.52207738595	− 0.52207738562	-0.52207738507	− 0.52207738430
1	− 1	− 0.56626910513	− 0.56626889798	− 0.56626869061	− 0.56626848302	− 0.56626827522
	0	− 0.56636325550	− 0.56636325539	− 0.56636325506	− 0.56636325451	− 0.56636325375
	1	− 0.56626910513	− 0.56626931207	− 0.56626951878	− 0.56626972528	− 0.56626993155
2	− 1	− 0.61088742922	− 0.61088722053	− 0.61088701162	− 0.61088680249	− 0.61088659314
	0	− 0.61098125301	− 0.61098125290	− 0.61098125258	− 0.61098125203	− 0.61098125128
	1	− 0.61088742922	− 0.61088763770	− 0.61088784596	− 0.61088805401	− 0.61088826184
3	− 1	− 0.65583700835	− 0.65583679812	− 0.65583658767	− 0.65583637700	− 0.65583616612
	0	− 0.65593049418	− 0.65593049408	− 0.65593049375	− 0.65593049322	− 0.65593049247
	1	− 0.65583700835	− 0.65583721837	− 0.65583742818	− 0.65583763777	− 0.65583784714
4	− 1	− 0.70111698560	− 0.70111677383	− 0.70111656185	− 0.70111634965	− 0.70111613724
	0	− 0.70121012237	− 0.70121012226	− 0.70121012194	− 0.70121012141	− 0.70121012067
	1	− 0.70111698560	− 0.70111719716	− 0.70111740850	− 0.70111761963	− 0.70111783055
5	− 1	− 0.74672653080	− 0.74672631750	− 0.74672610398	− 0.74672589026	− 0.74672567632
	0	− 0.74681930766	− 0.74681930755	− 0.74681930724	− 0.74681930671	− 0.74681930597
	1	− 0.74672653080	− 0.74672674389	− 0.74672695677	− 0.74672716944	− 0.74672738190
n	m	$\vec{B} = 0, \Phi_{AB} = 0$	$\vec{B} = 0, \Phi_{AB} = 2$	$\vec{B} = 0, \Phi_{AB} = 4$	$\vec{B} = 0, \Phi_{AB} = 6$	$\vec{B} = 0, \Phi_{AB} = 8$
0	0	− 0.52207738606	− 0.52207738606	− 0.52207738605	− 0.52207738604	− 0.52207738602
1	− 1	− 0.56626910513	− 0.56626913550	− 0.56626916587	− 0.56626919623	− 0.56626922659
	0	− 0.56636325550	− 0.56636325549	− 0.56636325549	− 0.56636325547	− 0.56636325546
	1	− 0.56626910513	− 0.56626907476	− 0.56626904438	− 0.56626901399	− 0.56626898360

Table 10 continued

n	m	$\vec{B}=0, \Phi_{AB}=0$	$\vec{B}=0, \Phi_{AB}=2$	$\vec{B}=0, \Phi_{AB}=4$	$\vec{B}=0, \Phi_{AB}=6$	$\vec{B}=0, \Phi_{AB}=8$
2	− 1	− 0.61088742922	− 0.61088745949	− 0.61088748975	− 0.61088752001	− 0.61088755026
	0	− 0.61098125301	− 0.61098125301	− 0.61098125300	− 0.61098125299	− 0.61098125297
	1	− 0.61088742922	− 0.61088739895	− 0.61088736868	− 0.61088733840	− 0.61088730811
3	− 1	− 0.65583700835	− 0.65583703851	− 0.65583706866	− 0.65583709881	0.655837128952
	0	− 0.65593049418	− 0.65593049418	− 0.65593049417	− 0.65593049416	− 0.65593049414
	1	− 0.65583700835	− 0.65583697819	− 0.65583694802	− 0.65583691785	− 0.65583688768
4	− 1	− 0.70111698560	− 0.70111701564	− 0.70111704568	− 0.70111707572	− 0.70111710575
	0	− 0.70121012237	− 0.70121012237	− 0.70121012236	− 0.70121012235	− 0.70121012233
	1	− 0.70111698560	− 0.70111695555	− 0.70111692550	− 0.70111689544	− 0.70111686538
5	− 1	− 0.74672653080	− 0.74672656073	− 0.74672659065	− 0.74672662057	− 0.74672665048
	0	− 0.74681930766	− 0.74681930766	− 0.74681930765	− 0.74681930764	− 0.74681930762
	1	− 0.74672653080	− 0.74672650087	− 0.74672647093	− 0.74672644099	− 0.74672641104
n	m	$\vec{B}=\Phi_{AB}=0$	$\vec{B}=\Phi_{AB}=2$	$\vec{B}=\Phi_{AB}=4$	$\vec{B}=\Phi_{AB}=6$	$\vec{B}=\Phi_{AB}=8$
0	0	− 0.52207738606	− 0.52207738598	− 0.52207738574	− 0.52207738535	− 0.52207738479
1	− 1	− 0.56626910513	− 0.56626892839	− 0.56626875148	− 0.56626857442	− 0.56626839721
	0	− 0.56636325550	− 0.56636325542	− 0.56636325518	− 0.56636325479	− 0.56636325424
	1	− 0.56626910513	− 0.56626928172	− 0.56626945816	− 0.56626963443	− 0.56626981055
2	− 1	− 0.61088742922	− 0.61088725083	− 0.61088707228	− 0.61088689357	− 0.61088671471
	0	− 0.61098125301	− 0.61098125293	− 0.61098125270	− 0.61098125232	− 0.61098125178
	1	− 0.61088742922	− 0.61088760747	− 0.61088778555	− 0.61088796349	− 0.61088814127
3	− 1	− 0.65583700835	− 0.65583682831	− 0.65583664811	− 0.65583646776	− 0.65583628726
	0	− 0.65593049418	− 0.65593049411	− 0.65593049388	− 0.65593049350	− 0.65593049297
	1	− 0.65583700835	− 0.65583718824	− 0.65583736798	− 0.65583754757	− 0.65583772701

Table 10 continued

n	m	$\vec{B} = \Phi_{AB} = 0$	$\vec{B} = \Phi_{AB} = 2$	$\vec{B} = \Phi_{AB} = 4$	$\vec{B} = \Phi_{AB} = 6$	$\vec{B} = \Phi_{AB} = 8$
4	− 1	− 0.70111698560	− 0.70111680391	− 0.70111662207	− 0.70111644007	− 0.70111625793
	0	− 0.70121012237	− 0.70121012230	− 0.70121012207	− 0.70121012170	− 0.70121012117
	1	− 0.70111698560	− 0.70111716714	− 0.70111734854	− 0.70111752978	− 0.70111771088
5	− 1	− 0.74672653080	− 0.74672634746	− 0.74672616397	− 0.74672598034	− 0.74672579655
	0	− 0.74681930766	− 0.74681930758	− 0.74681930736	− 0.74681930700	− 0.74681930648
	1	− 0.74672653080	− 0.74672671399	− 0.74672689704	− 0.74672707994	− 0.74672726269

Table 11 Energy eigenvalues spectrum of the GKP for H_2 molecule with different quantum numbers and magnetic field $B = 0$ for various values of the Φ_{AB},$q = 1$ with $a = -0.5$

n	m	$\Phi_{AB} = 0, \vec{B} = 0$	$\Phi_{AB} = 0, \vec{B} = 2$	$\Phi_{AB} = 0, \vec{B} = 4$	$\Phi_{AB} = 0, \vec{B} = 6$	$\Phi_{AB} = 0, \vec{B} = 8$
0	0	-0.51663513376	− 0.51663513374	− 0.51663513368	− 0.51663513357	− 0.51663513342
1	− 1	− 0.54901873681	− 0.54901745138	− 0.54901616590	− 0.54901488037	− 0.54901359479
	0	− 0.55575126519	− 0.55575126517	− 0.55575126508	− 0.55575126494	− 0.55575126475
	1	− 0.54901873681	− 0.54902002219	− 0.54902130752	− 0.54902259280	− 0.54902387803
2	− 1	− 0.60071532548	− 0.60071371783	− 0.60071211012	− 0.60071050235	− 0.60070889452
	0	− 0.60698075340	− 0.60698075337	− 0.60698075327	− 0.60698075311	− 0.60698075289
	1	− 0.60071532548	− 0.60071693308	− 0.60071854060	− 0.60072014809	− 0.60072175550
3	− 1	− 0.66340778725	− 0.66340588459	− 0.66340398186	− 0.66340207908	− 0.66340017623
	0	− 0.66925001772	− 0.66925001769	− 0.66925001759	− 0.66925001743	− 0.66925001719
	1	− 0.66340778725	− 0.66340968984	− 0.66341159238	− 0.66341349485	− 0.66341539726
4	− 1	− 0.73620730027	− 0.73620512537	− 0.73620295042	− 0.73620077540	− 0.73619860032
	0	− 0.74166381324	− 0.74166381321	− 0.74166381311	− 0.74166381295	− 0.74166381273
	1	− 0.73620730027	− 0.73620947510	− 0.73621164987	− 0.73621382458	− 0.73621599923
5	− 1	− 0.81836785165	− 0.81836542370	− 0.81836299569	− 0.81836056762	− 0.81835813950
	0	− 0.82347082806	− 0.82347082803	− 0.82347082795	− 0.82347082780	− 0.82347082760
	1	− 0.81836785165	− 0.81837027955	− 0.81837270739	− 0.81837513517	− 0.81837756290
n	m	$\vec{B} = 0, \Phi_{AB} = 0$	$\vec{B} = 0, \Phi_{AB} = 2$	$\vec{B} = 0, \Phi_{AB} = 4$	$\vec{B} = 0, \Phi_{AB} = 6$	$\vec{B} = 0, \Phi_{AB} = 8$
0	0	− 0.51663513376	− 0.51663513357	− 0.51663513301	− 0.51663513206	− 0.51663513074
1	− 1	− 0.54901873681	− 0.54902090542	− 0.54902307369	− 0.54902524161	− 0.54902740918
	0	− 0.55575126519	− 0.55575126502	− 0.55575126449	− 0.55575126362	− 0.55575126239
	1	− 0.54901873681	− 0.54901656785	− 0.54901439854	− 0.54901222888	− 0.54901005887
2	− 1	− 0.60071532548	− 0.60071734375	− 0.60071936170	− 0.60072137932	− 0.60072339661
	0	− 0.60698075340	− 0.60698075323	− 0.60698075274	− 0.60698075193	− 0.60698075079

Table 11 continued

n	m	$\vec{B}=0, \Phi_{AB}=0$	$\vec{B}=0, \Phi_{AB}=2$	$\vec{B}=0, \Phi_{AB}=4$	$\vec{B}=0, \Phi_{AB}=6$	$\vec{B}=0, \Phi_{AB}=8$
	1	− 0.60071532548	− 0.60071330689	− 0.60071128798	− 0.60070926874	− 0.60070724918
3	− 1	− 0.66340778725	− 0.66340966929	− 0.66341155102	− 0.66341343246	− 0.66341531359
	0	− 0.66925001772	− 0.66925001757	− 0.66925001711	− 0.66925001635	− 0.66925001529
	1	− 0.66340778725	− 0.66340590490	− 0.66340402226	− 0.66340213932	− 0.66340025607
4	− 1	− 0.73620730027	− 0.73620905813	− 0.73621081572	− 0.73621257302	− 0.73621433004
	0	− 0.74166381324	− 0.74166381310	− 0.74166381267	− 0.74166381196	− 0.74166381096
	1	− 0.73620730027	− 0.73620554212	− 0.73620378369	− 0.73620202498	− 0.73620026598
5	− 1	− 0.81836785165	− 0.81836949569	− 0.81837113947	− 0.81837278299	− 0.81837442624
	0	− 0.82347082806	− 0.82347082793	− 0.82347082753	− 0.82347082686	− 0.82347082593
	1	− 0.81836785165	− 0.81836620734	− 0.81836456277	− 0.81836291794	− 0.81836127284
n	m	$\vec{B}=\Phi_{AB}=0$	$\vec{B}=\Phi_{AB}=2$	$\vec{B}=\Phi_{AB}=4$	$\vec{B}=\Phi_{AB}=6$	$\vec{B}=\Phi_{AB}=8$
0	0	− 0.51663513376	− 0.51663513357	− 0.51663513301	− 0.51663513206	− 0.51663513074
1	− 1	− 0.55575126519	− 0.54902090542	− 0.54902307369	− 0.54902524161	− 0.54902740918
	0	− 0.55575126519	− 0.55575126502	− 0.55575126449	− 0.55575126362	− 0.55575126239
	1	− 0.54901873681	− 0.54901656785	− 0.54901439854	− 0.54901222888	− 0.54901005887
2	− 1	− 0.60071532548	− 0.60071734375	− 0.60071936170	− 0.60072137932	− 0.60072339661
	0	− 0.60698075340	− 0.60698075323	− 0.60698075274	− 0.60698075193	− 0.60698075079
	1	− 0.60071532548	− 0.60071330689	− 0.60071128798	− 0.60070926874	− 0.60070724918
3	− 1	− 0.66340778725	− 0.66340966929	− 0.66341155102	− 0.66341343246	− 0.66341531359
	0	− 0.66925001772	− 0.66925001757	− 0.66925001711	− 0.66925001635	− 0.66925001529
	1	− 0.66340778725	− 0.66340590490	− 0.66340402226	− 0.66340213932	− 0.66340025607

Table 11 continued

n	m	$\vec{B} = \Phi_{AB} = 0$	$\vec{B} = \Phi_{AB} = 2$	$\vec{B} = \Phi_{AB} = 4$	$\vec{B} = \Phi_{AB} = 6$	$\vec{B} = \Phi_{AB} = 8$
4	− 1	− 0.73620730027	− 0.73620905813	− 0.73621081572	− 0.73621257302	− 0.73621433004
	0	− 0.74166381324	− 0.74166381310	− 0.74166381267	− 0.74166381196	− 0.74166381096
	1	− 0.73620730027	− 0.73620554212	− 0.73620378369	− 0.73620202498	− 0.73620026598
5	− 1	− 0.81836785165	− 0.81836949569	− 0.81837113947	− 0.81837278299	− 0.81837442624
	0	− 0.82347082806	− 0.82347082793	− 0.82347082753	− 0.82347082686	− 0.82347082593
	1	− 0.81836785165	− 0.81836620734	− 0.81836456277	− 0.81836291794	− 0.81836127284

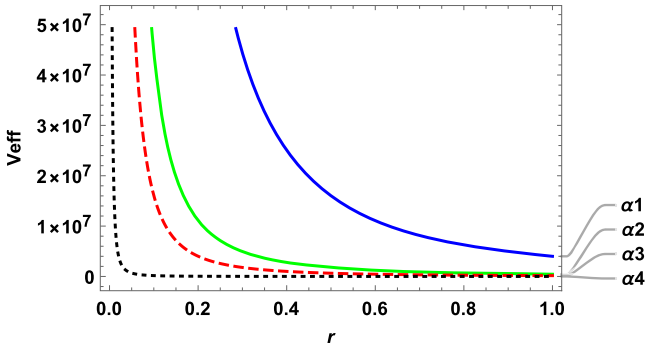

Fig. 1 The effective MYKP $(V_{eff}(r))$ *vs*. a function of the interatomic distance r for the parameters as $a_2 = A_1 = 2, A_2 = 4, \hbar = \mu = q = c = a = a_1 = 1, B = 2T, \Phi_{AB} = 2$ and magnetic quantum number $m = 0$ with various values of screening parameter α as $\alpha_1 = 0.001, \alpha_2 = 0.003, \alpha_3 = 0.005, \alpha_4 = 0.05\alpha_4 = 0.1$

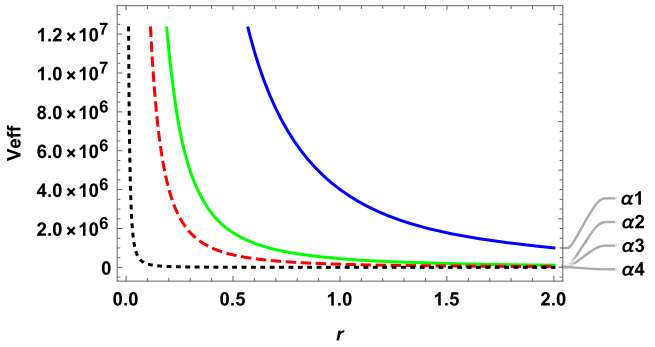

Fig. 2 The effective MYKP $(V_{eff}(r))$ *vs*. a function of the interatomic distance r for the parameters as $a_2 = A_1 = 2, A_2 = 4, \hbar = \mu = q = c = a = a_1 = 1, B = 2T, \Phi_{AB} = 2$ and magnetic quantum number $m = 1$ with various values of screening parameter α as $\alpha_1 = 0.001, \alpha_2 = 0.003, \alpha_3 = 0.005, \alpha_4 = 0.05\alpha_4 = 0.1$

energy eigenvalues of the various molecules, we used spectroscopic parameters given in Table 1.

Plots of the effective potential against interatomic distance r for various values of screening parameter α for $m = 0$, $m = 1$ and $m = -1$ presents in Figs. 1, 2 and 3 respectively. Effective potential decreases with increases r. Figures 4, 5 and 6 show the variation in effective potential with respect to magnetic field $\vec{B}$ for different values of α corresponds to $m = 0$, $m = 1$ and $m = -1$ presents respectively. Plots show effective potential increases with increases $\vec{B}$. Plots of the effective potential against Φ_{AB} for various values of screening parameter α for $m = 0$, $m = 1$ and $m = -1$ presents in Figs. 7, 8 and 9 respectively. Effective potential increases with increases Φ_{AB}.

Changes in energy eigenvalues with respect to screening parameter α for different values of the magnetic quantum numbers $m_0 = -2, m_2 = -1, m_3 = 0, m_4 = 1$ and $m_5 = 2$ for $n = 0$, $n = 1$ and $n = 2$ presents in Figs. 10, 11 and 12 respectively.

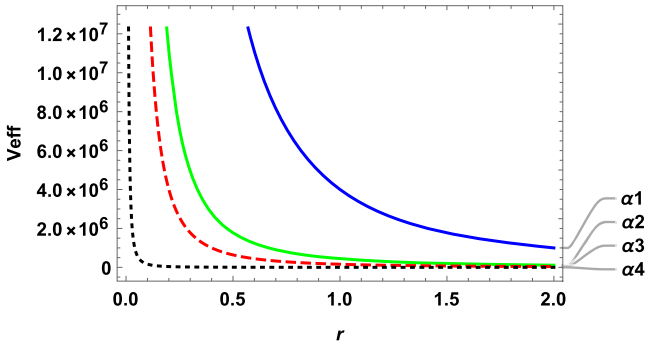

Fig. 3 The effective MYKP $(V_{eff}(r))$ *vs*. a function of the interatomic distance r for the parameters as $a_2 = A_1 = 2, A_2 = 4, \hbar = \mu = q = c = a = a_1 = 1, B = 2T, \Phi_{AB} = 2$ and magnetic quantum number $m = -1$ with various values of screening parameter α as $\alpha_1 = 0.001, \alpha_2 = 0.003, \alpha_3 = 0.005, \alpha_4 = 0.05\alpha_4 = 0.1$

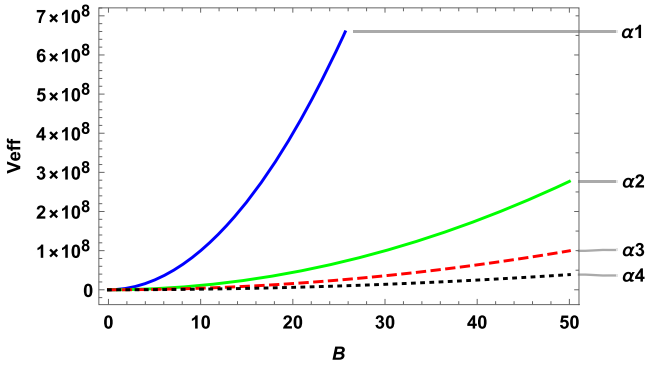

Fig. 4 The effective MYKP$(V_{eff}(r))$ against a function of magnetic field B for the parameters as $a_2 = A_1 = 1, A_2 = 2, \hbar = \mu = q = c = 1, r = 1, \Phi_{AB} = 2$ and magnetic quantum number $m = 0$ with various values of screening parameter α as $\alpha_1 = 0.001, \alpha_2 = 0.003, \alpha_3 = 0.005, \alpha_4 = 0.008$

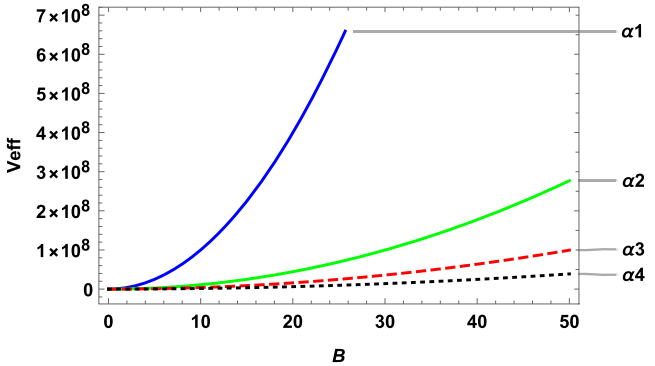

Fig. 5 The effective MYKP$(V_{eff}(r))$ against a function of magnetic field B for the parameters as $a_2 = A_1 = 1, A_2 = 2, \hbar = \mu = q = c = 1, r = 1, \Phi_{AB} = 2$ and magnetic quantum number $m = 1$ with various values of screening parameter α as $\alpha_1 = 0.001, \alpha_2 = 0.003, \alpha_3 = 0.005, \alpha_4 = 0.008$

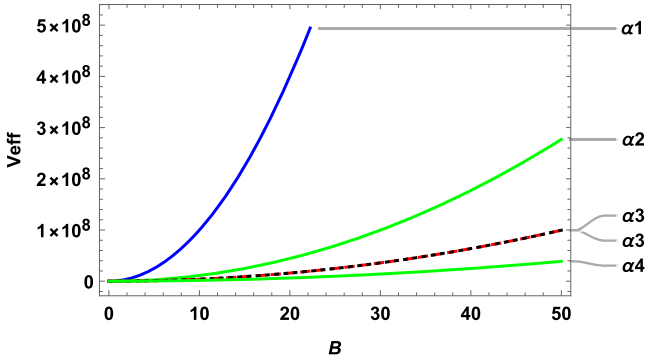

Fig. 6 The effective MYKP($V_{eff}(r)$) against a function of magnetic field B for the parameters as $a_2 = A_1 = 1, A_2 = 2, \hbar = \mu = q = c = 1, r = 1, \Phi_{AB} = 2$ and magnetic quantum number $m = -1$ with various values of screening parameter α as $\alpha_1 = 0.001, \alpha_2 = 0.003, \alpha_3 = 0.005, \alpha_4 = 0.008$

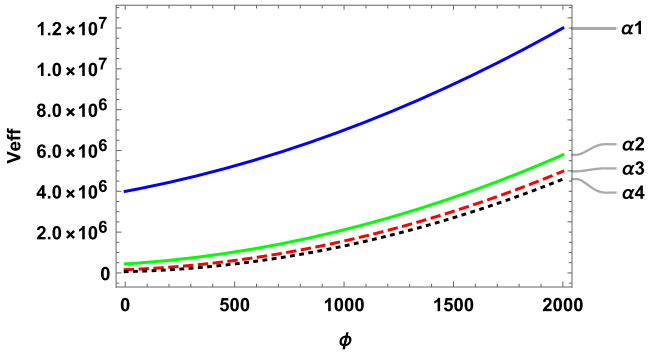

Fig. 7 The effective MYKP ($V_{eff}(r)$) against a function of AB flux field Φ_{AB} for the parameters as $a_2 = A_1 = 1, A_2 = 2, \hbar = \mu = q = c = 1, r = 1, B = 2$ and magnetic quantum number $m = 0$ with various values of screening parameter α as $\alpha_1 = 0.001, \alpha_2 = 0.003, \alpha_3 = 0.005, \alpha_4 = 0.008$

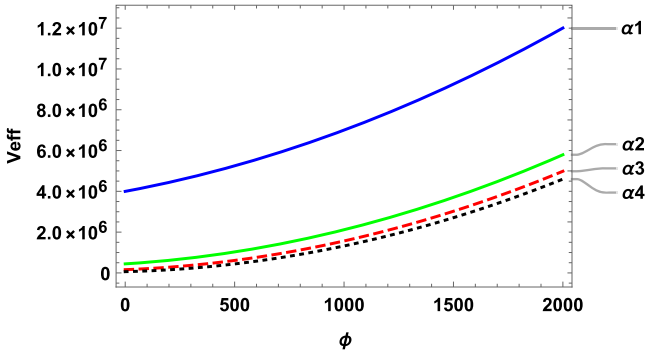

Fig. 8 The effective MYKP ($V_{eff}(r)$) against a function of AB flux field Φ_{AB} for the parameters as $a_2 = A_1 = 1, A_2 = 2, \hbar = \mu = q = c = 1, r = 1, B = 2$ and magnetic quantum number $m = 1$ with various values of screening parameter α as $\alpha_1 = 0.001, \alpha_2 = 0.003, \alpha_3 = 0.005, \alpha_4 = 0.008$

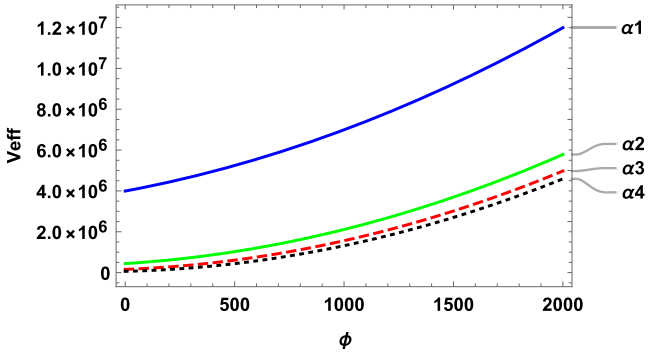

Fig. 9 The effective MYKP ($V_{eff}(r)$) against a function of AB flux field Φ_{AB} for the parameters as $a_2 = A_1 = 1, A_2 = 2, \hbar = \mu = q = c = 1, r = 1, B = 2$ and magnetic quantum number $m = -1$ with various values of screening parameter α as $\alpha_1 = 0.001, \alpha_2 = 0.003, \alpha_3 = 0.005, \alpha_4 = 0.008$

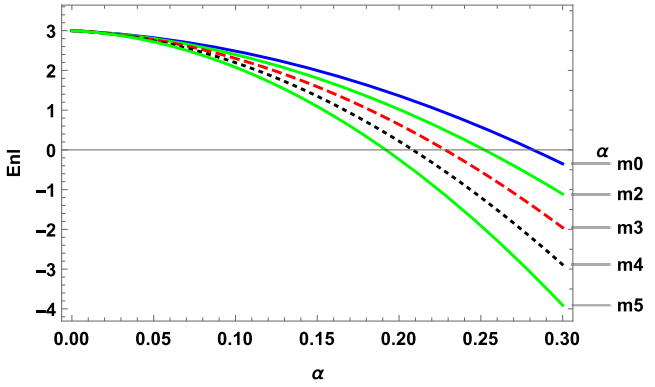

Fig. 10 The energy spectrum $E_{n\ell}$ for MYKP against a function of the screening parameter α for the parameters as $a_2 = A_1 = 2, A_2 = 4, \hbar = \mu = q = c = 1, r = 1, B = 5$ and quantum number $n = 0$ with various magnetic quantum number m as $m_0 = -2, m_2 = -1, m_3 = 0, m_4 = 1, m_5 = 2$

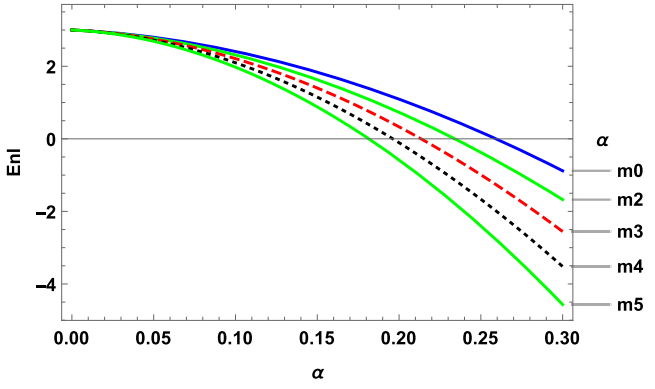

Fig. 11 The energy spectrum $E_{n\ell}$ for MYKP against a function of the screening parameter α for the parameters as $a_2 = A_1 = 2, A_2 = 4, \hbar = \mu = q = c = 1, r = 1, B = 5$ and quantum number $n = 1$ with various magnetic quantum number m as $m_0 = -2, m_2 = -1, m_3 = 0, m_4 = 1, m_5 = 2$

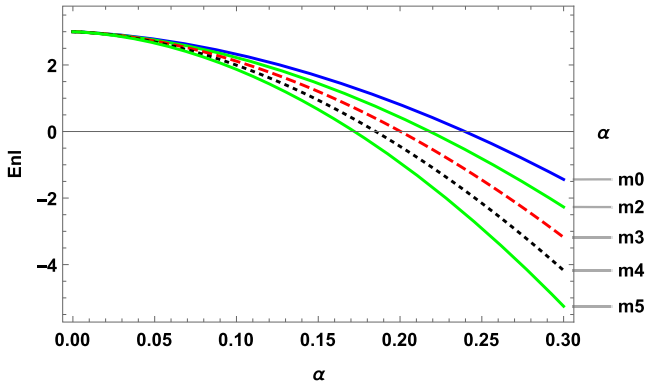

Fig. 12 The energy spectrum $E_{n\ell}$ for MYKP against a function of the screening parameter α for the parameters as $a_2 = A_1 = 2, A_2 = 4, \hbar = \mu = q = c = 1, r = 1, B = 5$ and quantum number $n = 2$ with various magnetic quantum number m as $m_0 = -2, m_2 = -1, m_3 = 0, m_4 = 1, m_5 = 2$

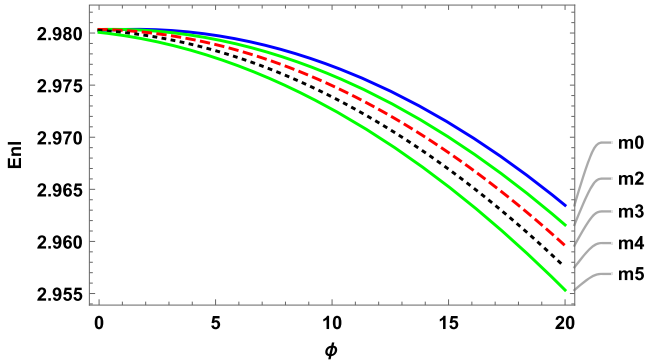

Fig. 13 The energy eigenvalues $E_{n\ell}$ for MYKP against a function of ϕ_{AB} for the parameters as $a_2 = A_1 = 2, A_2 = 4, \hbar = \mu = q = c = 1, \alpha = 0.01, B = 5$ and quantum number $n = 0$ with various values of the magnetic quantum number m as $m_0 = -2, m_2 = -1, m_3 = 0, m_4 = 1, m_5 = 2$

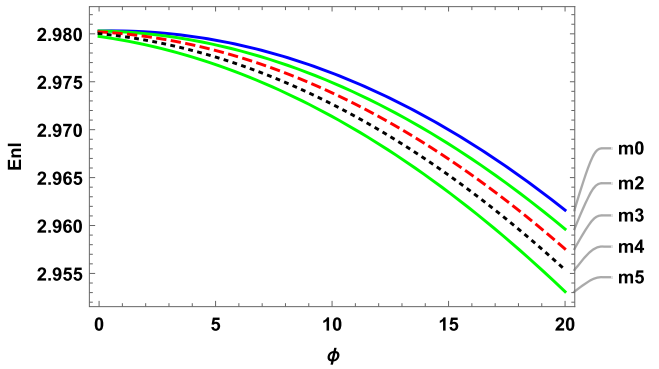

Fig. 14 The energy eigenvalues $E_{n\ell}$ for MYKP against a function of ϕ_{AB} for the parameters as $a_2 = A_1 = 2, A_2 = 4, \hbar = \mu = q = c = 1, \alpha = 0.01, B = 5$ and quantum number $n = 1$ with various values of the magnetic quantum number m as $m_0 = -2, m_2 = -1, m_3 = 0, m_4 = 1, m_5 = 2$

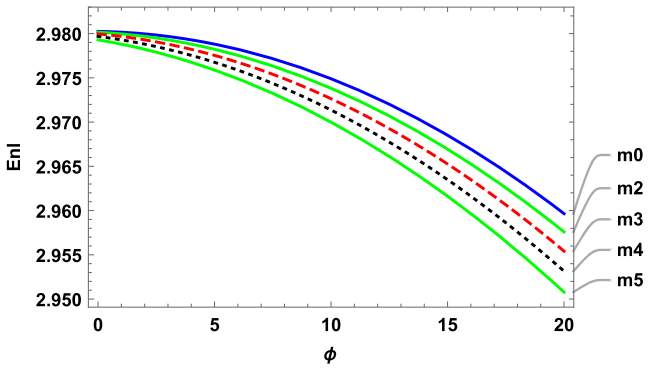

Fig. 15 The energy eigenvalues $E_{n\ell}$ for MYKP against a function of ϕ_{AB} for the parameters as $a_2 = A_1 = 2$, $A_2 = 4$, $\hbar = \mu = q = c = 1$, $\alpha = 0.01$, $B = 5$ and quantum number $n = 2$ with various values of the magnetic quantum number m as $m_0 = -2, m_2 = -1, m_3 = 0, m_4 = 1, m_5 = 2$

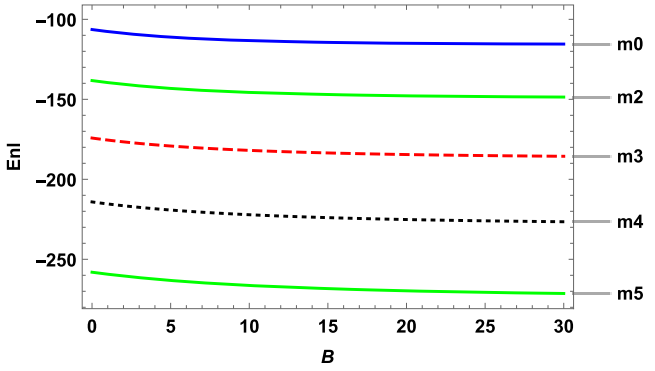

Fig. 16 The energy spectrum $E_{n\ell}$ for MYKP with respect to a function of B for the parameters as $a_2 = A_1 = 2$, $A_2 = 4$, $\hbar = \mu = q = c = 1$, $\alpha = 2$, $\Phi = 10$ and quantum number $n = 0$ with various values of the magnetic quantum number m as $m_0 = -2, m_2 = -1, m_3 = 0, m_4 = 1, m_5 = 2$

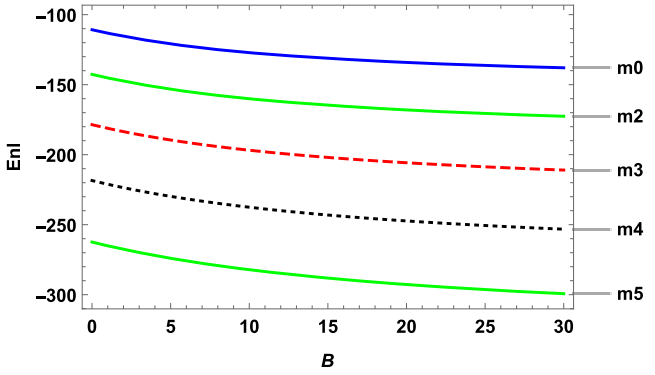

Fig. 17 The energy spectrum $E_{n\ell}$ for MYKP with respect to a function of B for the parameters as $a_2 = A_1 = 2$, $A_2 = 4$, $\hbar = \mu = q = c = 1$, $\alpha = 2$, $\Phi = 10$ and quantum number $n = 1$ with various values of the magnetic quantum number m as $m_0 = -2, m_2 = -1, m_3 = 0, m_4 = 1, m_5 = 2$

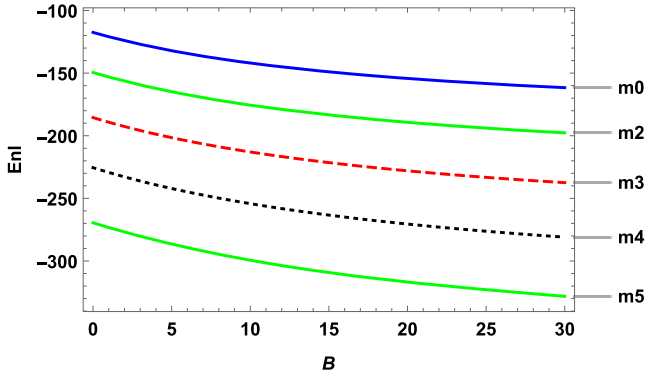

Fig. 18 The energy spectrum $E_{n\ell}$ for MYKP with respect to a function of B for the parameters as $a_2 = A_1 = 2$, $A_2 = 4$, $\hbar = \mu = q = c = 1$, $\alpha = 2$, $\Phi = 10$ and quantum number $n = 2$ with various values of the magnetic quantum number m as $m_0 = -2, m_2 = -1, m_3 = 0, m_4 = 1, m_5 = 2$

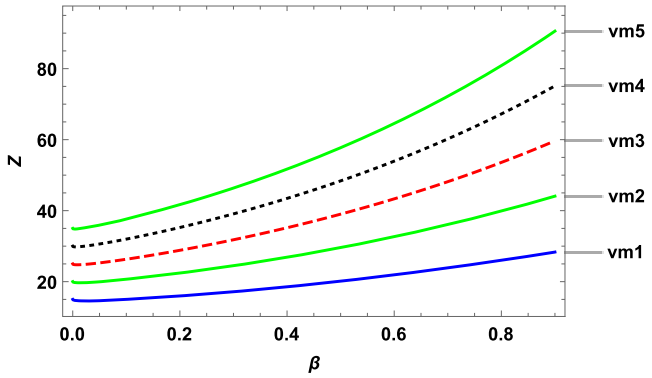

Fig. 19 The partition function (Z) of the MYKP $vs.$ a function of the temperature parameter β for the parameters as $a = \hbar = \mu = q = c = m = n = 1, a = 5, a_1 = 1, a_2 = 2, A_1 = 1.5, A_2 = 2.25, D_e = 3, \vec{B} = 5T, \Phi_{AB} = 20$ and $\alpha = 0.9$ with various vibrational quantum number υ_{max} as $\upsilon_{m1} = 15, \upsilon_{m2} = 20, \upsilon_{m3} = 25, \upsilon_{m4} = 30, \upsilon_{m5} = 35$ in two dimensions

Figures show energy eigenvalues decreases with increases α for MYKP. Variation in energy eigenvalues corresponds to Φ_{AB} for different values of the magnetic quantum numbers $m_0 = -2, m_2 = -1, m_3 = 0, m_4 = 1$ and $m_5 = 2$ for $n = 0, n = 1$ and $n = 2$ presents in Figs. 13, 14 and 15 respectively. Figures show energy eigenvalues decreases exponentially with increases Φ_{AB} for MYKP. Changes in energy eigenvalues corresponds to $\vec{B}$ for different values of the magnetic quantum numbers $m_0 = -2$, $m_2 = -1, m_3 = 0, m_4 = 1$ and $m_5 = 2$ for $n = 0, n = 1$ and $n = 2$ presents in Figs. 16, 17 and 18 respectively. Figures indicate that energy eigenvalues decreases slowly with increases $\vec{B}$ for MYKP.

Figure 19 shows the changes of the partition function with respect to temperature parameter β for the various values of the vibrational quantum number υ_{max}. The relationship in this case shows the partition function increases gradually as β increased. Changes in the partition function $Z(\vec{B}, \Phi_{AB}, \beta)$ corresponds to magnetic

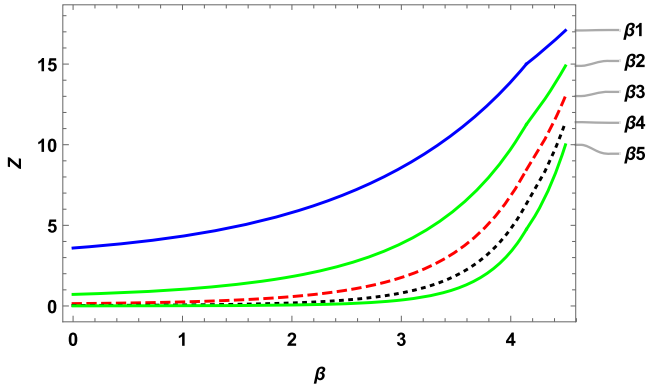

Fig. 20 The partition function (Z) of the MYKP $vs.$ a function of the magnetic field $\vec{B}$ (in Tesla) for the parameters as $a = \hbar = \mu = q = c = m = n = 1, a = 5, a_1 = 1, a_2 = 2, A_1 = 1.5, A_2 = 2.25, D_e = 3, \upsilon_{max} = 20, \Phi_{AB} = 20$ and $\alpha = 0.9$ with various temperature parameter β as $\beta_1 = 0.1, \beta_2 = 0.2, \beta_3 = 0.3, \beta_4 = 0.4, \beta_5 = 0.5$ in two dimensions

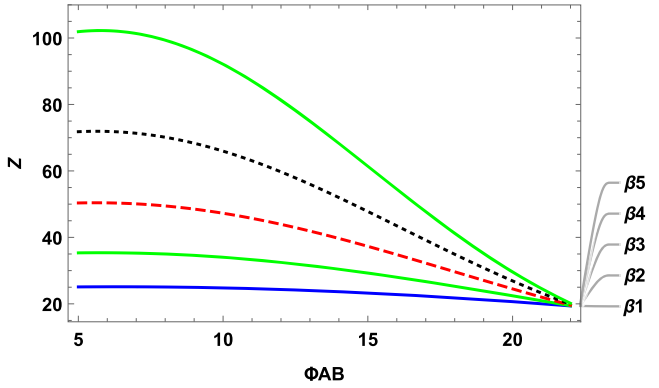

Fig. 21 The partition function (Z) of the MYKP $vs.$ a function of the Aharanov-Bohm flux field Φ_{AB} for the parameters as $a = \hbar = \mu = q = c = m = n = 1, a = 5, a_1 = 1, a_2 = 2, A_1 = 1.5, A_2 = 2.25, D_e = 3, \upsilon_{max} = 20, \vec{B} = 5T$ and $\alpha = 0.9$ with various temperature parameter β as $\beta_1 = 0.1, \beta_2 = 0.2, \beta_3 = 0.3, \beta_4 = 0.4, \beta_5 = 0.5$

field $\vec{B}$ for different values of the β is presents in the Fig. 20. Plots show that initially the $Z(\vec{B}, \Phi_{AB}, \beta)$ increases slowly as $\vec{B}$ increased and after $\vec{B} = 3T$, the partition function increases an exponentially with $\vec{B}$. Figure 21 illustrates the variation of the $Z(\vec{B}, \Phi_{AB}, \beta)$ with AB flux field Φ_{AB} for different values of the β. It is clearly shown in these plots that the partition function decreases slowly as increasing Φ_{AB} and tends to $Z(\vec{B}, \Phi_{AB}, \beta) = 0$ around $\Phi_{AB} = 22$. In Fig. 22, we shows the behaviour of the internal energy $U(\vec{B}, \Phi_{AB}, \beta)$ with respect to β for different values of the υ_{max}. Plots show that internal energy decreases monotonically as decreasing β. Variation in internal energy $U(\vec{B}, \Phi_{AB}, \beta)$ corresponds to magnetic field $\vec{B}$ for various values of the β presented in Fig. 23 We noted that $U(\vec{B}, \Phi_{AB}, \beta)$ initially increases and after $vecB = 9T$ its decreases monotonically for $\beta = 0.08$ and 0.09 whereas U decreases linearly as $\vec{B}$ increased for $\beta = 0.8$ and 0.9. Changes in internal

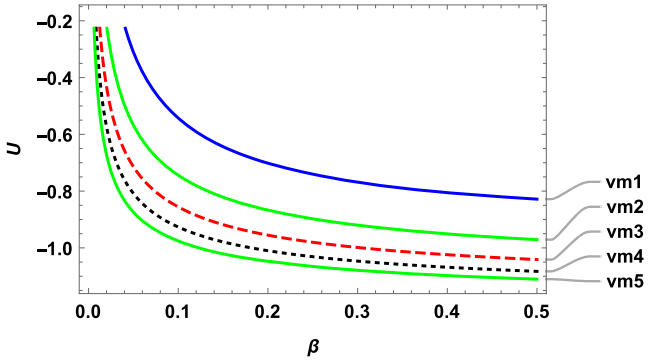

Fig. 22 The internal energy U of the MYKP against a function of the temperature parameter β for the parameters as $a = \hbar = \mu = q = c = m = n = 1, a = 5, a_1 = 1, a_2 = 2, A_1 = 1.5, A_2 = 2.25, D_e = 3, \vec{B} = 5T, \Phi_{AB} = 20$ and $\alpha = 0.9$ with various vibrational quantum number υ_{max} as $\upsilon_{m1} = 15, \upsilon_{m2} = 20, \upsilon_{m3} = 25, \upsilon_{m4} = 30, \upsilon_{m5} = 35$ in two dimensions

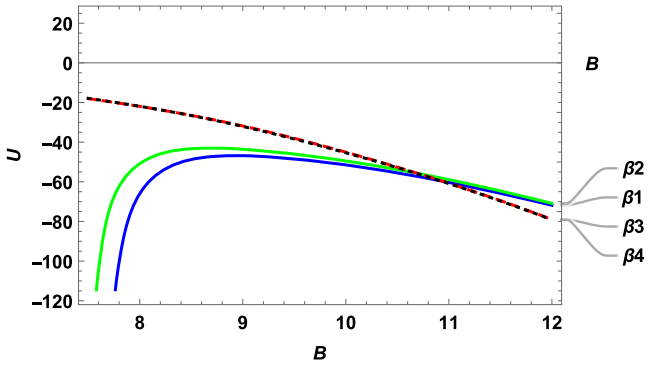

Fig. 23 The internal energy U of the MYKP against a function of the magnetic field $\vec{B}$ for the parameters as $\hbar = \mu = q = c = m = n = 1, a = 5, a_1 = 1, a_2 = 2, A_1 = 1.5, A_2 = 2.25, D_e = 3, \upsilon_{max} = 10, \Phi_{AB} = 20$ and $\alpha = 0.9$ with various temperature parameter β as $\beta_1 = 0.08, \beta_2 = 0.09, \beta_3 = 0.8, \beta_4 = 0.9$ in two dimensions

energy $U(\vec{B}, \Phi_{AB}, \beta)$ with respect to AB flux field Φ_{AB} for various values of the β presented in Fig. 24 shows $U(\vec{B}, \Phi_{AB}, \beta)$ deceases initially and increases gradually after $\Phi_{AB} = 6$ as Φ_{AB} increased. Variation of the free energy $F(\vec{B}, \Phi_{AB}, \beta)$ with varying β corresponds to different values of the vibrational quantum number υ_{max} shows in Fig. 25. It is shown that free energy increases exponentially with increasing β. In Fig. 26, we shows the changes in $F(\vec{B}, \Phi_{AB}, \beta)$ with respect to magnetic field $\vec{B}$ for various values of the temperature parameter β. It is clearly seen that $F(\vec{B}, \Phi_{AB}, \beta)$ decreases gradually with increasing $\vec{B}$. In Fig. 27, we shows behaviour of the free energy $F(\vec{B}, \Phi_{AB}, \beta)$ with respect to AB flux field Φ_{AB} for different values of the temperature parameter β. The figure clearly indicates the $F(\vec{B}, \Phi_{AB}, \beta)$ decreases slowly as AB flux field increased. Figure 28 shows the changes of the entropy $S(\vec{B}, \Phi_{AB}, \beta)$ with respect to temperature parameter β for different values of the vibrational quantum number υ_{max}. We shows entropy decreases monotonically as

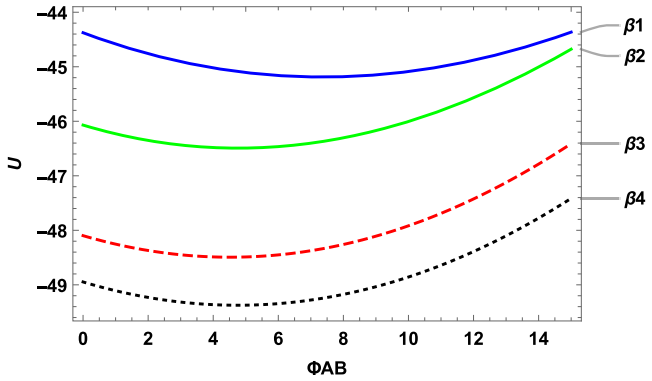

Fig. 24 The internal energy U of the MYKP against a function of the Aharanov-Bohm flux field Φ_{AB} for the parameters as $\hbar = \mu = q = c = m = n = 1, a = 5, a_1 = 1, a_2 = 2, A_1 = 1.5, A_2 = 2.25, D_e = 3, \upsilon_{max} = 10, \vec{B} = 10T$ and $\alpha = 0.9$ with various temperature parameter β as $\beta_1 = 0.2, \beta_2 = 0.4, \beta_3 = 0.6, \beta_4 = 0.8$ in two dimensions

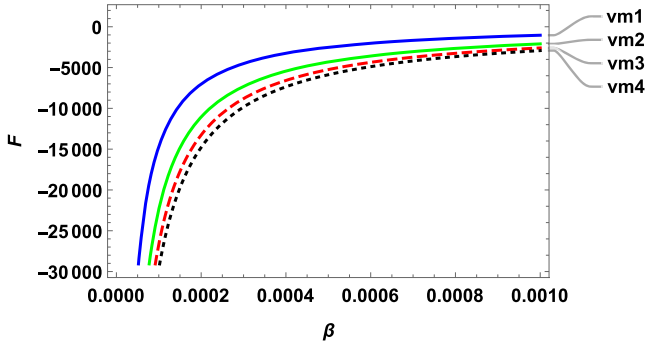

Fig. 25 The free energy F of the MYKP $vs.$ a function of the temperature parameter β for the parameters as $\hbar = \mu = q = c = m = n = 1, a = 5, a_1 = 1, a_2 = 2, A_1 = 1.5, A_2 = 2.25, D_e = 3, \vec{B} = 10T, \Phi_{AB} = 10$ and $\alpha = 0.9$ with various vibrational quantum number υ_{max} as $\upsilon_{m1} = 5, \upsilon_{m2} = 10, \upsilon_{m3} = 15, \upsilon_{m4} = 20$ in two dimensions

temperature parameter increased. Behavior of the entropy $S(\vec{B}, \Phi_{AB}, \beta)$ corresponds to magnetic field $\vec{B}$ with various values of the temperature parameter β shows in Fig. 29. it is clearly seen that entropy decreases gradually as increasing $\vec{B}$ for constant values of the remaining parameters. In Fig. 30, variation of the entropy $S(\vec{B}, \Phi_{AB}, \beta)$ with respect to AB flux field Φ_{AB} for different values of the β is presented. Plots show entropy abruptly decreases initially and remain almost constant for $\Phi_{AB} = 50$ to 65 after that it is suddenly increases as Φ_{AB} increased. We shows the behavior of the specific heat capacity $C_v(\vec{B}, \Phi_{AB}, \beta)$ with respect to temperature parameter β corresponds to various values of the vibrational quantum number υ_{max} in Fig. 31 We noted that specific heat capacity increases as increasing temperature parameter. In Fig. 32 the variation of the specific heat capacity $C_v(\vec{B}, \Phi_{AB}, \beta)$ corresponds to magnetic field $\vec{B}$ for different values of the temperature parameter β is presented. The plots show that $C_v(\vec{B}, \Phi_{AB}, \beta)$ decreases exponentially and $C_v(\vec{B}, \Phi_{AB}, \beta)$ reaches

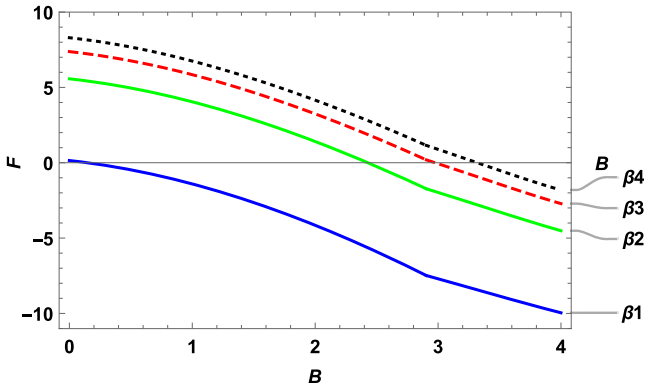

Fig. 26 The free energy F of the MYKP vs.a function of the magnetic field $\vec{B}$ for the parameters as $\hbar = \mu = q = c = m = n = 1, a = 5, a_1 = 1, a_2 = 2, A_1 = 1.5, A_2 = 2.25, D_e = 3, \upsilon_{max} = 10, \Phi_{AB} = 10$ and $\alpha = 0.9$ with various temperature parameter β as $\beta_1 = 0.2, \beta_2 = 0.4, \beta_3 = 0.6, \beta_4 = 0.8$ in two dimensions

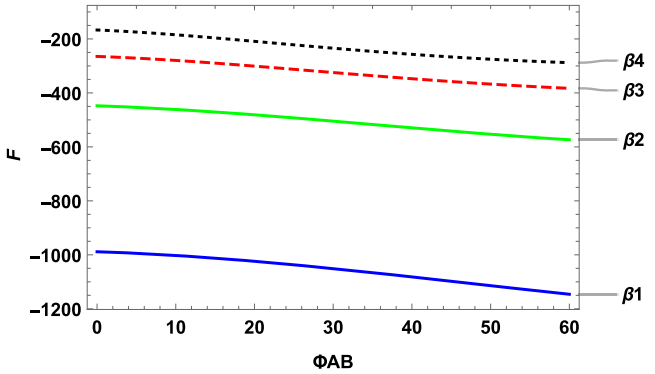

Fig. 27 The free energy F of the MYKP vs. a function of the Aharanov-Bohm flux field Φ_{AB} for the parameters as $\hbar = \mu = q = c = m = n = 1, a = 5, a_1 = 1, a_2 = 2, A_1 = 1.5, A_2 = 2.25, D_e = 3, \upsilon_{max} = 10, \vec{B} = 10T$ and $\alpha = 0.9$ with various temperature parameter β as $\beta_1 = 0.2, \beta_2 = 0.4, \beta_3 = 0.6, \beta_4 = 0.8$ in two dimensions

zero for all plots at $\vec{B} = 2.9$ after that it is increases linearly as increasing β. Figure 33 shows the behavior of the specific heat capacity $C_v(\vec{B}, \Phi_{AB}, \beta)$ with respect to AB flux field Φ_{AB} for different values of the temperature parameter β. The plots show that specific heat capacity initially decreases monotonically and later increases suddenly as AB flux field increased. Variation in the magnetization $M(\vec{B}, \Phi_{AB}, \beta)$ at finite temperature with temperature parameter β for various values of the vibrational quantum number υ_{max} presented in Fig. 34 Plots show magnetization decreases monotonically for vibrational quantum number $\upsilon_{m2} = 10, \upsilon_{m3} = 15, \upsilon_{m4} = 20$ and for vibrational quantum number $\upsilon_{m1} = 5$, magnetization almost remained constant as increasing β. Figure 35 shows changes of the magnetization $M(\vec{B}, \Phi_{AB}, \beta)$ at finite temperature with magnetic field $\vec{B}$ corresponds to different values of the temperature parameter β. The plots seen that magnetization increases with $\vec{B}$ increased. In

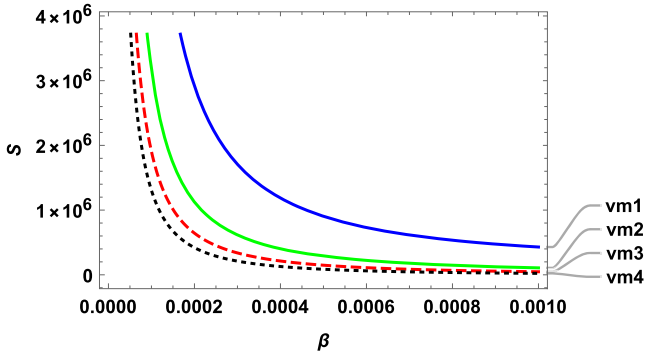

Fig. 28 The entropy S of the MYKP $vs.$ a function of the temperature parameter β for the parameters as $\hbar = \mu = q = c = m = n = 1, a = 5, a_1 = 1, a_2 = 2, A_1 = 1.5, A_2 = 2.25, D_e = 3, \vec{B} = 10T, \Phi_{AB} = 10$ and $\alpha = 0.9$ with various vibrational quantum number υ_{max} as $\upsilon_{m1} = 5, \upsilon_{m2} = 10, \upsilon_{m3} = 15, \upsilon_{m4} = 20$ in two dimensions

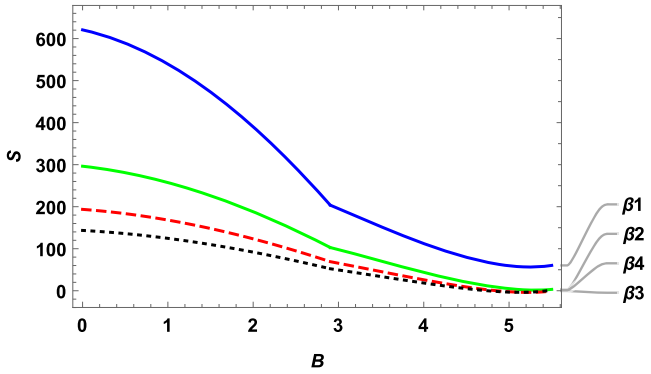

Fig. 29 The entropy S of the MYKP $vs.$a function of the magnetic field $\vec{B}$ for the parameters as $\hbar = \mu = q = c = m = n = 1, a = 5, a_1 = 1, a_2 = 2, A_1 = 1.5, A_2 = 2.25, D_e = 3, \upsilon_{max} = 10, \Phi_{AB} = 10$ and $\alpha = 0.9$ with various temperature parameter β as $\beta_1 = 0.2, \beta_2 = 0.4, \beta_3 = 0.6, \beta_4 = 0.8$ in two dimensions

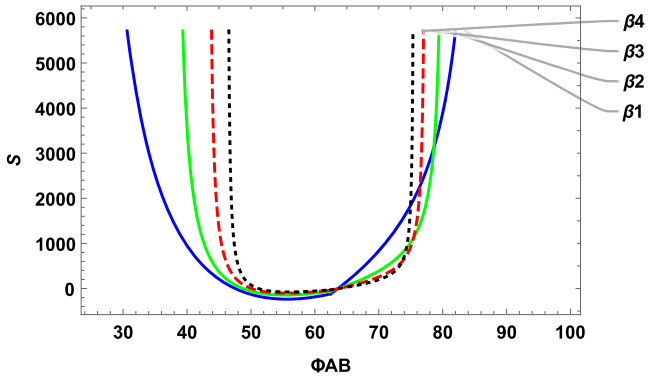

Fig. 30 The entropy S of the MYKP $vs.$ a function of the Aharanov-Bohm flux field Φ_{AB} for the parameters as $\hbar = \mu = q = c = m = n = 1, a = 5, a_1 = 1, a_2 = 2, A_1 = 1.5, A_2 = 2.25, D_e = 3, \upsilon_{max} = 10, \vec{B} = 10T$ and $\alpha = 0.9$ with various temperature parameter β as $\beta_1 = 0.2, \beta_2 = 0.4, \beta_3 = 0.6, \beta_4 = 0.8$ in two dimensions

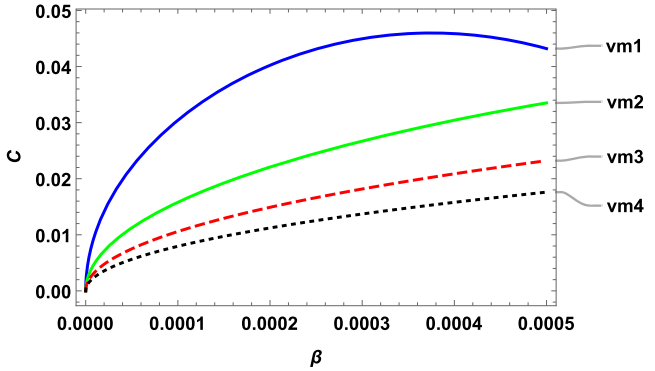

Fig. 31 The specific heat capacity C_v of the MYKP $vs.$ a function of the temperature parameter β for the parameters as $\hbar = \mu = q = c = m = n = 1, a = 5, a_1 = 1, a_2 = 2, A_1 = 1.5, A_2 = 2.25, D_e = 3, \vec{B} = 10T, \Phi_{AB} = 10$ and $\alpha = 0.9$ with various vibrational quantum number υ_{max} as $\upsilon_{m1} = 5, \upsilon_{m2} = 10, \upsilon_{m3} = 15, \upsilon_{m4} = 20$ in two dimensions

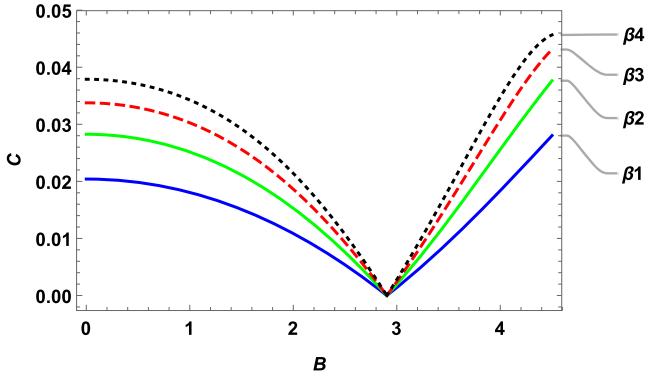

Fig. 32 The specific heat capacity C_v of the MYKP $vs.$a function of the magnetic field $\vec{B}$ for the parameters as $\hbar = \mu = q = c = m = n = 1, a = 5, a_1 = 1, a_2 = 2, A_1 = 1.5, A_2 = 2.25, D_e = 3, \upsilon_{max} = 10, \Phi_{AB} = 10$ and $\alpha = 0.9$ with various temperature parameter β as $\beta_1 = 0.02, \beta_2 = 0.04, \beta_3 = 0.06, \beta_4 = 0.08$ in two dimensions

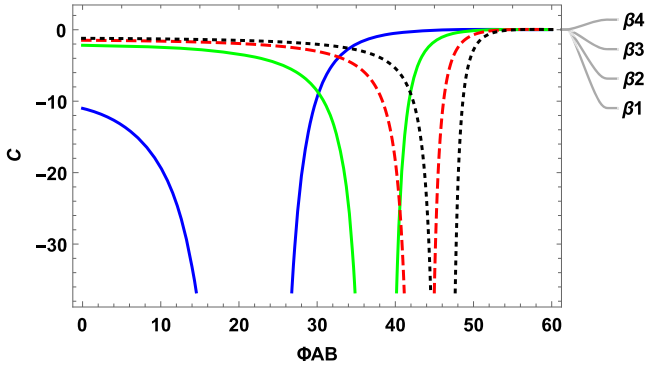

Fig. 33 The specific heat capacity C_v of the MYKP $vs.$ a function of the Aharanov-Bohm flux field Φ_{AB} for the parameters as $\hbar = \mu = q = c = m = n = 1, a = 5, a_1 = 1, a_2 = 2, A_1 = 1.5, A_2 = 2.25, D_e = 3, \upsilon_{max} = 10, \vec{B} = 10T$ and $\alpha = 0.9$ with various temperature parameter β as $\beta_1 = 0.02, \beta_2 = 0.04, \beta_3 = 0.06, \beta_4 = 0.08$ in two dimensions

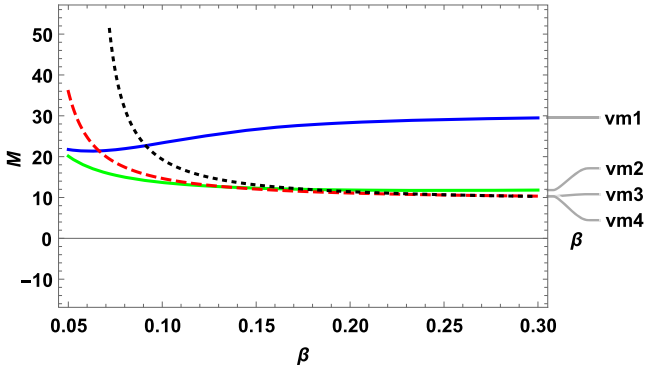

Fig. 34 The magnetization M of the MYKP $vs.$ a function of the temperature parameter β for the parameters as $\hbar = \mu = q = c = m = n = 1, a = 5, a_1 = 1, a_2 = 2, A_1 = 1.5, A_2 = 2.25, D_e = 3, \vec{B} = 10T, \Phi_{AB} = 10$ and $\alpha = 0.9$ with various vibrational quantum number υ_{max} as $\upsilon_{m1} = 5, \upsilon_{m2} = 10, \upsilon_{m3} = 15, \upsilon_{m4} = 20$ in two dimensions

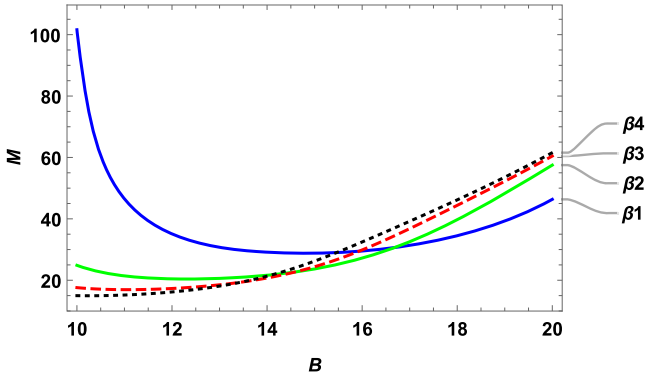

Fig. 35 The magnetization M of the MYKP $vs.$a function of the magnetic field $\vec{B}$ for the parameters as $\hbar = \mu = q = c = m = n = 1, a = 5, a_1 = 1, a_2 = 2, A_1 = 1.5, A_2 = 2.25, D_e = 3, \upsilon_{max} = 10, \Phi_{AB} = 10$ and $\alpha = 0.9$ with various temperature parameter β as $\beta_1 = 0.02, \beta_2 = 0.04, \beta_3 = 0.06, \beta_4 = 0.08$ in two dimensions

Fig. 36 we shows behaviour of the magnetization $M(\vec{B}, \Phi_{AB}, \beta)$ at finite temperature against AB flux field Φ_{AB} for various values of the temperature parameter β. These plots show magnetization decreases with increasing Φ_{AB}. Behaviour of the magnetic susceptibility $\chi_m(\vec{B}, \Phi_{AB}, \beta)$ at finite temperature with temperature parameter β for various values of the vibrational quantum number υ_{max} is presented in Fig. 37 We observe that magnetic susceptibility increases slowly with β increased. In Fig. 38 we shows the variation of the magnetic susceptibility $\chi_m(\vec{B}, \Phi_{AB}, \beta)$ at finite temperature with varying magnetic field $\vec{B}$ corresponds to different values of the β. We noted that magnetic susceptibility increases randomly with $\vec{B}$ increased. Variation in the magnetic susceptibility $\chi_m(\vec{B}, \Phi_{AB}, \beta)$ at finite temperature against AB flux field Φ_{AB} for different values of the temperature parameter β is presented in Fig. 39 We notice that the magnetic susceptibility decreases slowly with increasing Φ_{AB} for temperature parameter $\beta_1 = 0.002$ and temperature parameter $\beta_2 = 0.004$ whereas the magnetic

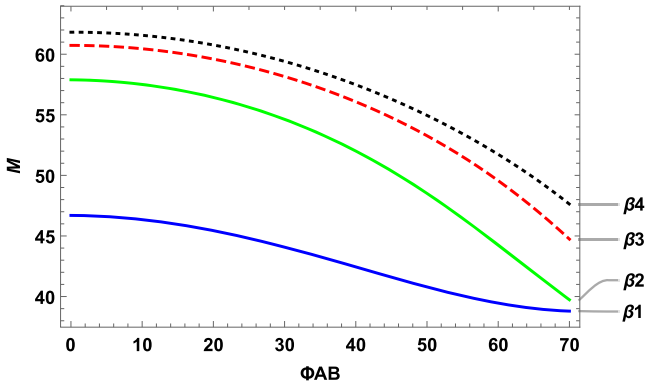

Fig. 36 The magnetization M of the MYKP $vs.$ a function of the Aharanov-Bohm flux field Φ_{AB} for the parameters as $\hbar = \mu = q = c = m = n = 1, a = 5, a_1 = 1, a_2 = 2, A_1 = 1.5, A_2 = 2.25, D_e = 3, \upsilon_{max} = 10, \vec{B} = 20T$ and $\alpha = 0.9$ with various temperature parameter β as $\beta_1 = 0.02, \beta_2 = 0.04, \beta_3 = 0.06, \beta_4 = 0.08$ in two dimensions

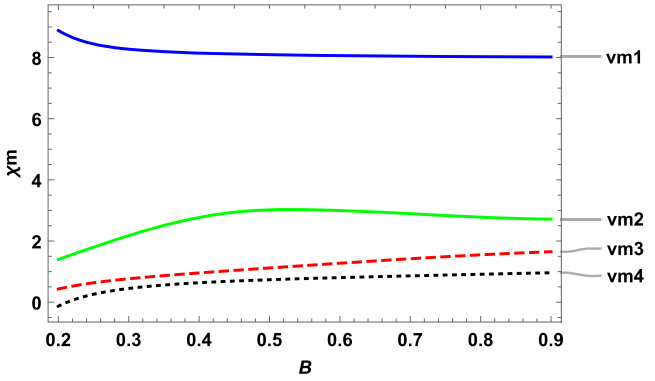

Fig. 37 The magnetic susceptibility χ_m of the MYKP $vs.$ a function of the temperature parameter β for the parameters as $\hbar = \mu = q = c = m = n = 1, a = 5, a_1 = 1, a_2 = 2, A_1 = 1.5, A_2 = 2.25, D_e = 3, \vec{B} = 10T, \Phi_{AB} = 10$ and $\alpha = 0.9$ with various vibrational quantum number υ_{max} as $\upsilon_{m1} = 5, \upsilon_{m2} = 10, \upsilon_{m3} = 15, \upsilon_{m4} = 20$ in two dimensions

susceptibility almost remained const with increasing Φ_{AB} for temperature parameter $\beta_3 = 0.006$ and temperature parameter $\beta_4 = 0.008$.

6 Conclusions

The energy spectrum for MYKP with the magnetic field and Aharanov–Bohm flux field was obtained using the pNU approach and SEM in this study. There are special cases for the GKP, MKP, KP, and HP. The MYKP, KP, HP, MKP, and GKP numerical results are tabulated. The numerical results calculated for KP and HP are congruent with those obtained by others. There are many plots of the effective potential that correlate to interatomic distance r, magnetic field $\vec{B}$, and Aharanov–Bohm flux field Φ_{AB}. The energy eigenvalues are displayed with respect to the screening parameter

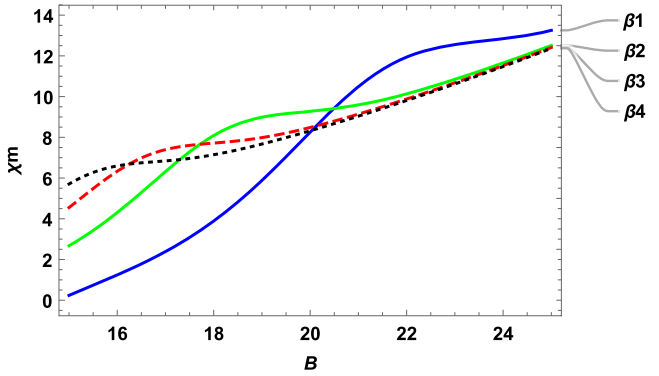

Fig. 38 The magnetic susceptibility χ_m of the MYKP vs.a function of the magnetic field $\vec{B}$ for the parameters as $\hbar = \mu = q = c = m = n = 1, a = 5, a_1 = 1, a_2 = 2, A_1 = 1.5, A_2 = 2.25, D_e = 3, \upsilon_{max} = 10, \Phi_{AB} = 10$ and $\alpha = 0.9$ with various temperature parameter β as $\beta_1 = 0.02, \beta_2 = 0.04, \beta_3 = 0.06, \beta_4 = 0.08$ in two dimensions

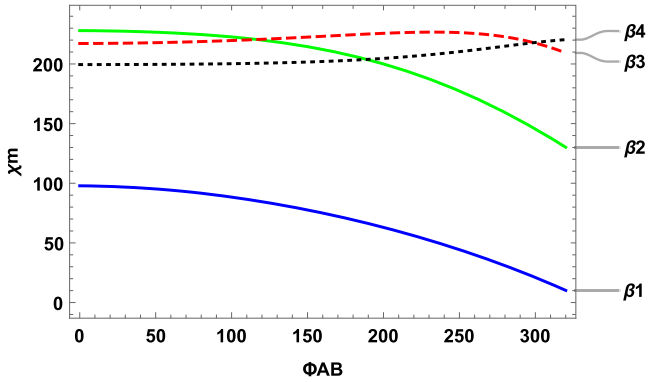

Fig. 39 The magnetic susceptibility χ_m of the MYKP vs. a function of the Aharanov-Bohm flux field Φ_{AB} for the parameters as $\hbar = \mu = q = c = m = n = 1, a = 5, a_1 = 1, a_2 = 2, A_1 = 1.5, A_2 = 2.25, D_e = 3, \upsilon_{max} = 10, \vec{B} = 10T$ and $\alpha = 0.09$ with various temperature parameter β as $\beta_1 = 0.002, \beta_2 = 0.004, \beta_3 = 0.006, \beta_4 = 0.008$ in two dimensions

α, the magnetic field $\vec{B}$, and the Aharanov-Bohm flux field Φ_{AB}. We also obtained and analysed additional thermodynamic parameters such as mean energy, mean free energy, entropy, and specific heat capacity using this information. Magnetization and magnetic susceptibility at finite temperatures under the effect of external fields were also discussed. We were able to discover additional physical chemical properties in position spaces under the MYKP by using the eigenfunction of the MYKP, including Gibbs free energy, bond length, Tsallis entropy, Renyi entropy, and Fisher information entropy. This article findings may be useful in atomic-molecular physics, solid-state physics, and physical chemistry.

Author Contributions KRP: Numerical calculation and graphical representation. RHP: Methodology and obtained solution of the MYKP with the magnetic field and Aharanov–Bohm flux field. AKR: Results–discussion and conclusions.

References

1. M. Eshshi, H. Mehraban, Eur. Phys. J. Plus **132**, 121 (2017)
2. M. Eshshi, H. Mehraban, S.M. Ikhdair, Eur. Phys. J. A **52**, 201 (2016)
3. H. Hassanabadi, E. Maghsoodi, S. Zarrinkamar, Ann. Phys. (Berlin) (2013). https://doi.org/10.1002/andp.2013001202
4. S.M. Ikhadiar, B.J. Falaye, J. Ass, Arab Univ Bas. App. Sci. (2013). https://doi.org/10.1006/j.jaubas.2013.07.004
5. K.R. Purohit, R.H. Parmar, A.K. Rai, Eur. Phys. J. Plus. **135**, 286 (2020)
6. R.H. Parmar, Eur. Phys. J. Plus. **134**, 86 (2019)
7. A.F. Nikiforov, V.B. Uvarov, *Special Functions of Mathematical Physics* (Birkhauser, Basel, 1988)
8. H. Hassanabadi, H. Rahimov, S. Zarrinkamar, Adv. High Energy Phys. **2011**, 458087 (2011)
9. Z.Q. Ma, B.W. Xu, Int. J. Mod. Phys. E **14**, 599 (2005)
10. S.H. Dong, A. Gonzalez-Cisneros, Ann. Phys. **323**, 1136 (2008)
11. S.H. Dong, Int. J. Quant. Chem. **109**, 701 (2009)
12. W.C. Qiang, S.H. Dong, EPL (Euro Phys. Lett.) **89**, 10003 (2010)
13. B.J. Falaye, K.J. Oyewumi, S.M. Ikhdair, M. Hamzavi, Phys. Script. **89**, 115204 (2014)
14. O. Bayrak, I. Boztosun, H. Ciftci, Int. J. Quantum Chem. **107**, 540 (2007)
15. S.H. Dong, *Factorization Method in Quantum Mechanics* (Springer, Cham, 2007)
16. A. Arda, R. Sever, Commun. Theor. Phys. **58**, 27 (2012)
17. J. Cai, P. Cai, A. Inomata, Phys. Rev. A **34**, 4621 (1986)
18. F. Cooper, A. Khare, U. Sukhatme, Phys. Rep. **251**, 267–365 (1995)
19. R.H. Parmar, Indian J. Phys. **93**(9), 1163–1170 (2019)
20. C. Yin, Z. Cao, Q. Shen, Ann. Phys. **325**, 528 (2010)
21. E.E. Ibekwe, U.S. Okorie, J.B. Emah, E.P. Inyang, S.A. Ekong, Eur. Phys. J. Plus. **136**, 87 (2021)
22. B. Aalu, Physica B **575**, 411699 (2019)
23. Y. Meir, O. Entin-Wohlman, Y. Gefen, Phys. Rev. B **42**, 8351 (1990)
24. B.I. Halperin, Phys. Rev. B **25**, 2185 (1982)
25. M.V. Berry, J.P. Keating, J. Phys. A **27**, 6167 (1994)
26. Y. Avishai, Y. Hatsugai, M. Kohmoto, Phys. Rev. B **47**, 9501 (1993)
27. U.F. Keyser, S. Borck, R.J. Haug, M. Bichler, G. Abstreiter, W. Wegscheider, Semicond. Sci. Technol. **17**, 22 (2002)
28. A.N. Ikot, U.S. Okorie, G. Osobonye, P.O. Amadi, C.O. Edet, M.J. Sithole, G.J. Rampho, R. Sever, Heliyon **6**, 03738 (2020)
29. A.N. Ikot, C.O. Edet, P.O. Amadi, U.S. Okorie, G.J. Rampho, H.Y. Abdullah, Eur. Phys. J. **74**, 159 (2020)
30. S.M. Ikhdair, M. Hamzavi, R. Sever, Physica B **407**, 4523–4529 (2012)
31. S.M. Ikhdair, M. Hamzavi, Physica B **407**, 4198–4207 (2012)
32. M. Hamzavi, S.M. Ikhdair, K.E. Thylwe, Zeitschrift fur Naturforschung A. **67**, 567–571 (2012)
33. R. Kumar, F. Chand, Phys. Scr. **85**(5), 055008–055004 (2012)
34. R. Kumar, F. Chand, Phys. Scr. **86**(2), 027001 (2012)
35. S.M. Ikhdair, B.J. Falaye, M. Hamzavi, Ann. Phys. **353**, 282–298 (2015)
36. E.E. Ibekwe, A.T. Ngiangia, U.S. Okorie, A.N. Ikot, H.Y. Abdullah, Iran J. Sci. Technol. **44**, 1191 (2020)
37. A.K. Rai, B. Patel, P.C. Vinodkumar, Phy. Rev. C **78**(5), 1 (2008)
38. A.K. Rai, J.N. Pandya, P.C. Vinodkumar, J. Phys. G **31**(12), 1453 (2005)
39. V. Kher, A.K. Rai, Chin. Phys. C **42**(8), 1–8 (2018)
40. R. Chaturvedi, A.K. Rai, Int. J. Theo. Phys. **59**, 3508 (2020)
41. E. Omugbe, O.E. Osafile, M.C. Hindawi, Adv. High Energy Phys. (2020). https://doi.org/10.1155/2020/5901464
42. M. Abu-Shady, T. Abdel-Karim, E. Khokha, Sci Fed J. Quant. Phys. **2**(1), 58 (2018)

43. E.E. Ibekwe, U.S. Okorie, J.B. Emah, E.P. Inyang, S.A. Ekong, Eur. Phys. J. Plus **87**, 136 (2021)
44. R. Rani, S.B. Hardwar, F. Chand, Commun. Theor. Phys. **70**, 179 (2018)
45. M. Abu-Shady, Sh.Y. Ezz, Few-Body Syst. **60**, 66 (2019)
46. R. Kumar, C. Fakir, Commun. Theor. Phys. **59**, 528 (2013)
47. K.R. Purohit, R.H. Parmar, A.K. Rai, Ann. Phys. **424**, 168335 (2021)
48. R.H. Parmar, P.C. Vinodkumar, J. Math. Chem. **59**, 1638–1703 (2021)
49. C. Tezcan, R. Sever, Int. J. Theor. Phys. **48**(2), 337 (2009)
50. W.C. Qiang, S.H. Dong, Phys. Lett. A **368**, 13–17 (2007)
51. M. Eshghi, R. Sever, S.M. Ikhdair, Chin. Phys. B **27**, 020301 (2018)
52. R.L. Greene, C. Aldrich, Phys. Rev. A **14**, 2363–2366 (1976)
53. M. Abramowitz, I.A. Stegun, *Handbook of Mathematical Functions with Formulas, Graphs and Mathematical Tables* (Dover, New York, 1964)
54. R. Rani, F. Chand, Ind. J. Phys. **92**(145), 1–7 (2018)
55. S.M. Ikhdair, R. Sever, J. Math. Chem. **45**(1137), 18 (2009)
56. I. Nasserl, M.S. Abdelmonem, Phys. Scr. **83**, 055004 (2011)
57. A.A. Rajabi, M. Hamzavi, Can. J. Phys. **91**, 5 (2013)
58. M. Hamzavi, K.E. Thylwe, A.A. Rajabi, Commun. Theor. Phys. **60**, 1 (2013)
59. C.A. Onate, M.C. Onyeaju, A.N. Ikot, O. Ebomwonyi, Eur. Phys. J. Plus **132**, 462 (2017)
60. C.A. Onate, J.O. Ojonubah, A. Adeoti, E.J. Eweh, M. Ugboja, Afr. Rev. Phys. **9**, 0062 (2014)
61. S.M. Ikhdair, R. Sever, J. Mol. Struct. **809**, 103 (2007)
62. A.N. Ikot, W. Azogor, U.S. Okorie, F.E. Bazuaye, M.C. Onjeaju, C.A. Onate, E.O. Chukwuocha, Indian J. Phys. (2019). https://doi.org/10.1007/s12648-019-01375-0
63. M. Toutounji, Int. J. Quant. Chem. **111**, 1885 (2011)
64. J.F. Wang, X.L. Peng, L.H. Zhang, C.W. Wang, C.S. Jia, Chem. Phys. Lett. **686**, 131 (2017)
65. U.S. Okorie, A.N. Ikot, M.C. Onyeaju, E.O. Chukwuocha, J. Mol. Model. **24**, 289 (2018)
66. A.N. Ikot, U.S. Okorie, R. Sever, G.J. Rampho, Eur. Phys. J. Plus **134**, 386 (2019)
67. X.Q. Song, C.W. Wang, C.S. Jia, Chem. Phys. Lett. **673**, 50 (2017)